NJC

New Journal of Chemistry

A journal for new directions in chemistry

Accepted Manuscript

This article can be cited before page numbers have been issued, to do this please use: S. S N C, S. Palawat and A. T. Paul, *New J. Chem.*, 2020, DOI: 10.1039/D0NJ02622K.

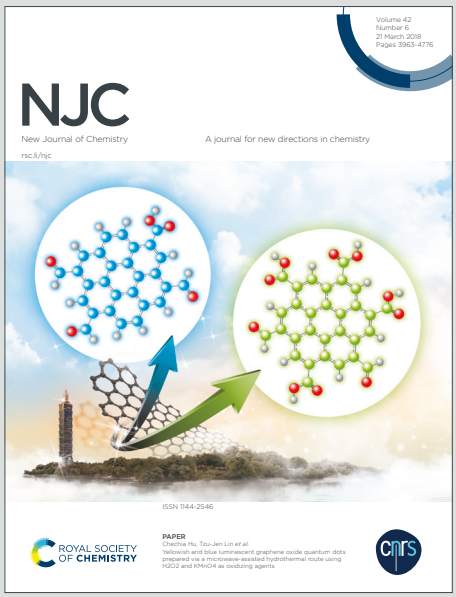

This is an Accepted Manuscript, which has been through the Royal Society of Chemistry peer review process and has been accepted for publication.

Accepted Manuscripts are published online shortly after acceptance, before technical editing, formatting and proof reading. Using this free service, authors can make their results available to the community, in citable form, before we publish the edited article. We will replace this Accepted Manuscript with the edited and formatted Advance Article as soon as it is available.

You can find more information about Accepted Manuscripts in the Information for Authors.

Please note that technical editing may introduce minor changes to the text and/or graphics, which may alter content. The journal's standard Terms & Conditions and the Ethical guidelines still apply. In no event shall the Royal Society of Chemistry be held responsible for any errors or omissions in this Accepted Manuscript or any consequences arising from the use of any information it contains.

View Article Online
DOI: 10.1039/D0NJ02622K

Title Page

Title:

Design, Synthesis, Biological Evaluation and Molecular Modelling Studies of Conophylline Inspired Novel Indolyl Oxoacetamides as Potent Pancreatic Lipase Inhibitors

Authors:

Sridhar S. N. C.[#], Saksham Palawat[#], Atish T. Paul[*].

[#] Equal contributing authors

[*] Corresponding author

Affiliations:

Laboratory of Natural Product Chemistry, Department of Pharmacy, Birla Institute of Technology and Science, Pilani (BITS Pilani), Pilani campus, Pilani - 333 031, Rajasthan, India.

Present Address:

Dr. Atish T. Paul,

Assistant Professor and Head,

Department of Pharmacy,

Birla Institute of Technology and Science, Pilani (Pilani Campus),

Pilani - 333 031, Rajasthan, India.

Email: atish.paul@pilani.bits-pilani.ac.in

View Article Online
DOI: 10.1039/D0NJ02622K

Abstract

A novel series of 21 indolyl oxoacetamide analogues were designed based on the natural product lead, conophylline, and evaluated for their pancreatic lipase inhibitory activity using porcine pancreatic lipase (Type II). Analogues **12c** and **12b** exhibited comparatively greater potential (IC_{50} values of 2.95 and 3.26 µM) than conophylline (IC_{50} - 3.31 µM) while the standard drug, orlistat exhibited potent IC_{50} value of 0.99 µM. Further, analogues **12b** and **12c** exhibited reversible competitive inhibition similar to orlistat and conophylline, and possessed K_i values of 1.89 and 1.69 µM, respectively. Molecular docking of these analogues was in agreement with the *in vitro* results, wherein the MolDock scores exhibited significant correlation with their inhibitory activity. A 10 ns molecular dynamics simulation of **12c** complexed with pancreatic lipase, confirmed the role of extended alkyl interactions along with π- π stacking and π-cation interactions, in stabilising the ligand in the active site (maximum observed RMSD ≈ 3.5 Å). ADMET prediction indicated the GI absorption of these analogues to be high, however, they did not possess carcinogenicity and hepatotoxicity in contrast to orlistat and conophylline.

Keywords

ADMET, Conophylline, Indolyl Oxoacetamides, Inhibition Kinetics, Molecular Dynamics, Pancreatic Lipase

View Article Online
DOI: 10.1039/D0NJ02622K

1. Introduction

Obesity is a chronic, relapsing, progressive, multifactorial metabolic disease characterized by excessive or abnormal accumulation of fat deposits in the body.[1–3] Worldwide, obesity has tripled since 1975 with recent reports from the World Health Organization (WHO) indicating a rapid upsurge in obese population. As per the recent WHO statistics, over 1.9 billion adults were found to be overweight, of which 650 million adults were found obese.[4] While obesity is preventable and does not itself impose any risk to the health, a chronic condition might lead to severe comorbid risks including insulin resistance, diabetes mellitus (Type II), hypertension, dyslipidaemia, coronary heart disease, sleep apnea, gall bladder disease, gout, osteoarthritis, and certain cancers.[5]

To date, around 15 drugs are approved for the treatment of obesity, however, a majority of these drugs are directed towards reducing the appetite, and would result in an overall inhibition of nutrition intake. On the contrary, orlistat (**1,** Figure 1), a β-lactone containing lipstatin derivative, acts through reversible covalent inhibition of pancreatic lipase (PL), and is widely prescribed for long term obesity treatment.[6,7] While, orlistat was reported to exhibit tolerable side effects *viz.*, steatorrhea, oily stools and frequent bowel movements, recent reports from FDA has cited severe adverse effects with long term administration of orlistat, that included hepatotoxicity, acute pancreatitis, gall stones and renal injuries.[8,9] These events have highlighted the necessity for safer and effective anti-obesity drugs.

In the recent years, various amide functionality-based pharmacophores, including tripeptides and rhodanines, were reported to exhibit potential PL inhibition.[10–12] The carbonyl groups of these amides mimic that of the natural esters in the triglycerides, thus acting as electrophiles for Ser 152 of the active site of PL. Previously, we have identified conophylline (**2,** Figure 1) from the leaves of *Tabernaemontana divaricata* as a potential natural product lead for PL inhibition.[13,14] Conophylline, a bis-indole alkaloid, exhibited an IC_{50} of 3.31 μM, comparable to that of orlistat (IC_{50} - 0.99 μM). Nevertheless, the lower PL inhibitory potential of conophylline in comparison to orlistat was attributed to the lack of a highly reactive carbonyl group in contrary to orlistat, and its structural rigidity yielding in high degree of unfavourable steric interactions with the active site of Human PL (Figures 1 and 2). Consequent studies that involved the use of molecular hybridization and scaffold hopping techniques resulted in various carbazolyl and indolyl oxoacetamides with potential PL inhibitory activity.[10,15,16] The α-ketoamide warhead of these oxoacetamides mimicked the function of the orlistat's β-lactone, while the unfavourable steric interactions were significantly reduced (Figures 3 and 4). In

addition, these studies also established the pivotal role of π-π stackings and π-cation interaction with the aromatic acids of the lid domain and Arg 256 respectively, for potential PL inhibition.

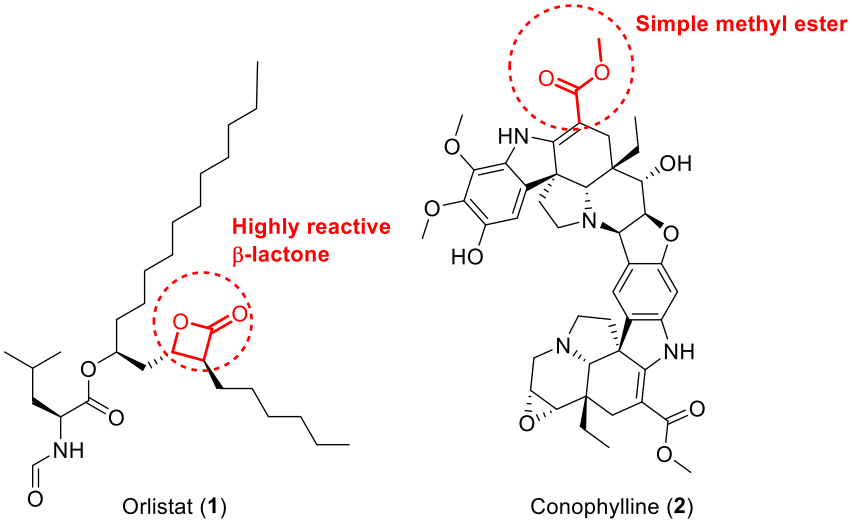

Fig. 1 Structures of Orlistat (**1**) and Conophylline (**2**) highlighting their respective reactive carbonyl groups

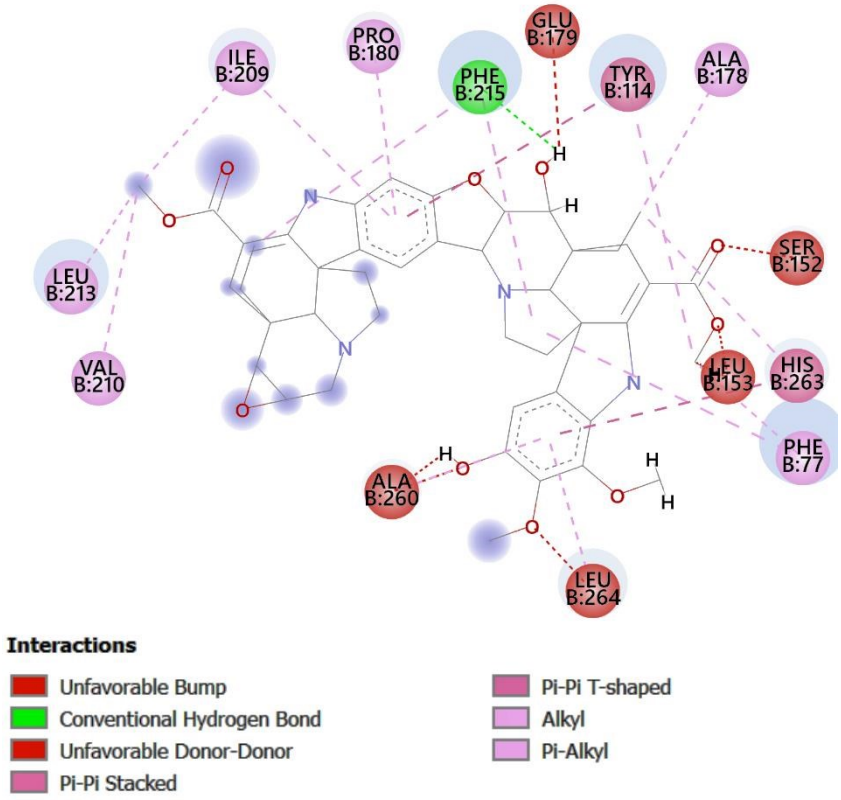

Fig. 2 2D pose of Conophylline (**2**) highlighting the unfavourable steric interactions (in red)

Nevertheless, the most potent indolyl oxoacetamide (**5**) exhibited lower, yet comparable PL inhibitory potential (IC_{50} - 4.53 μM) in comparison to conophylline (Figure 3). On the contrary, compound **5** that possessed a 5-methoxy substitution on the indole, did not exhibit

significant difference in its activity compared to its unsubstituted counterpart, **4** (IC_{50} = 4.92 μM), clearly indicating negligible role of 5-methoxy substitution.[10,16] The lower PL inhibitory potential of these indolyl oxoacetamides in comparison to conophylline was attributed to their minimal hydrophobic interactions (alkyl/π-alkyl) with the lid domain amino acids (Figure 4). Considering all the above facts, we hypothesized further developments to the indolyl oxoacetamides, with particular emphasis on its hydrophobic density and π-cation interactions, would result in potent PL inhibitors.

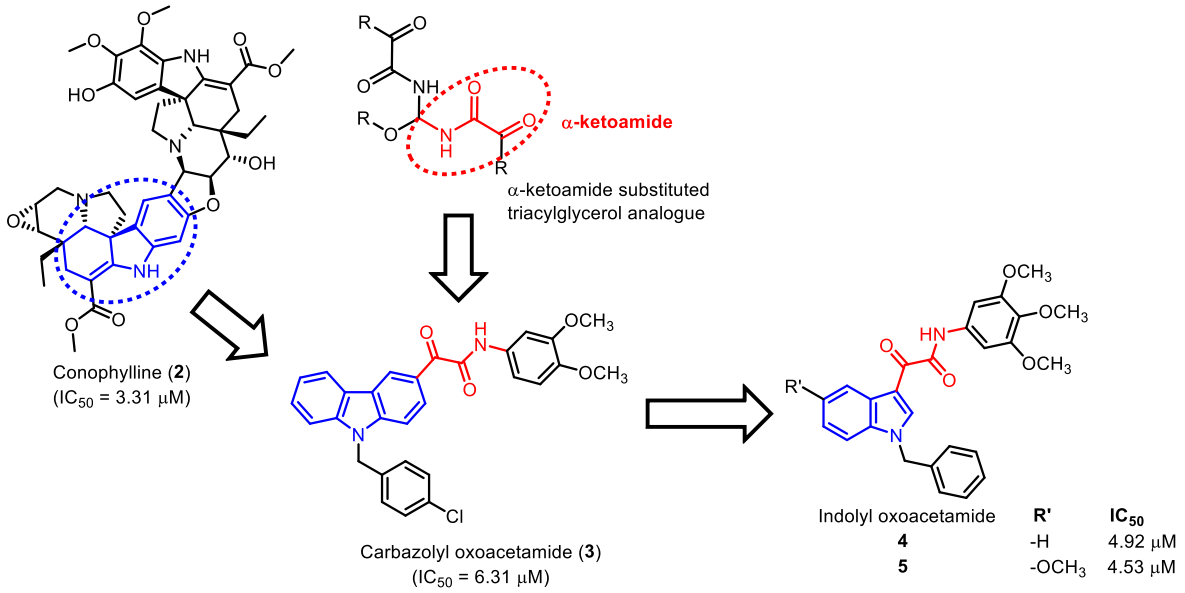

Fig. 3 Schematic representation indicating the series of events in designing the indolyl oxoacetamides

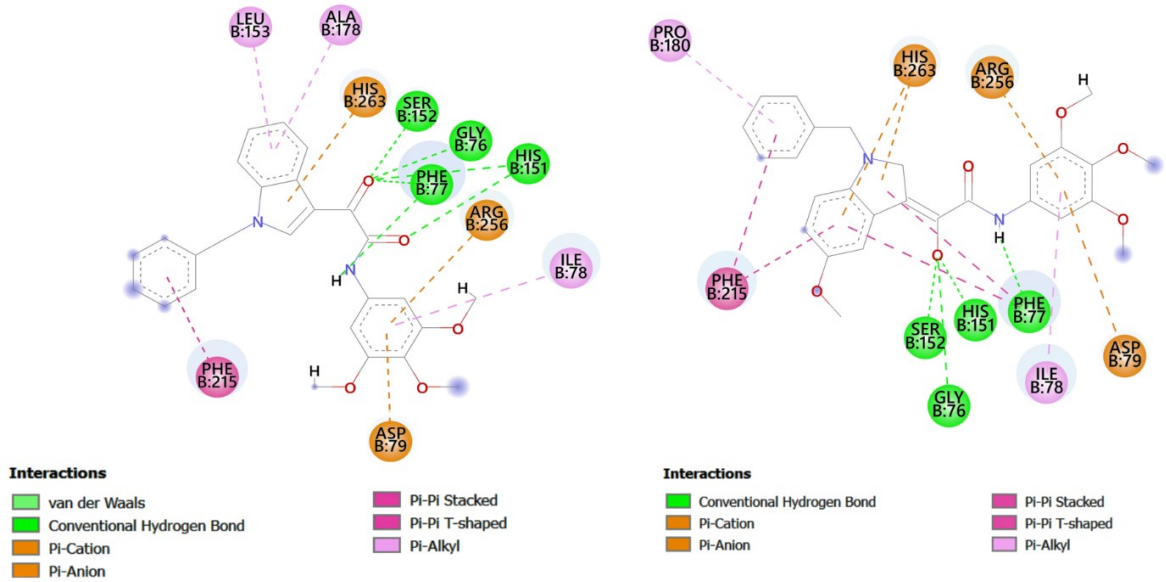

Fig. 4 2D interactions of compound **4** (left) and **5** (right) with Human PL, highlighting no unfavourable bumps and minimal π-alkyl interactions

View Article Online
DOI: 10.1039/D0NJ02622K

2. Results and discussion

2.1. Chemistry

A detailed literature review of various natural products-based PL inhibitors indicated the presence of prenyl and geranyl substitutions in potent PL inhibition.[6] Hence, in the present study, various indolyl oxoacetamides with N-prenyl and N-geranyl substitutions on the indole moiety were considered, along with N-ethyl, N-benzyl and the unsubstituted analogues. Further, literature reports suggested that the presence of heteroaryl groups can result in better π-cation interaction in comparison to the simple aryl groups.[17] Moreover, the presence of linker between the aryl extension and the amide, as observed in our previous studies, resulted in enhanced PL inhibitory activity.[10,16] Accordingly, trimethoxybenzyl and 2-(1H-indol-3-yl)ethyl substitutions were considered for the aryl extension (Ar), apart from various other substitutions (Scheme 1).

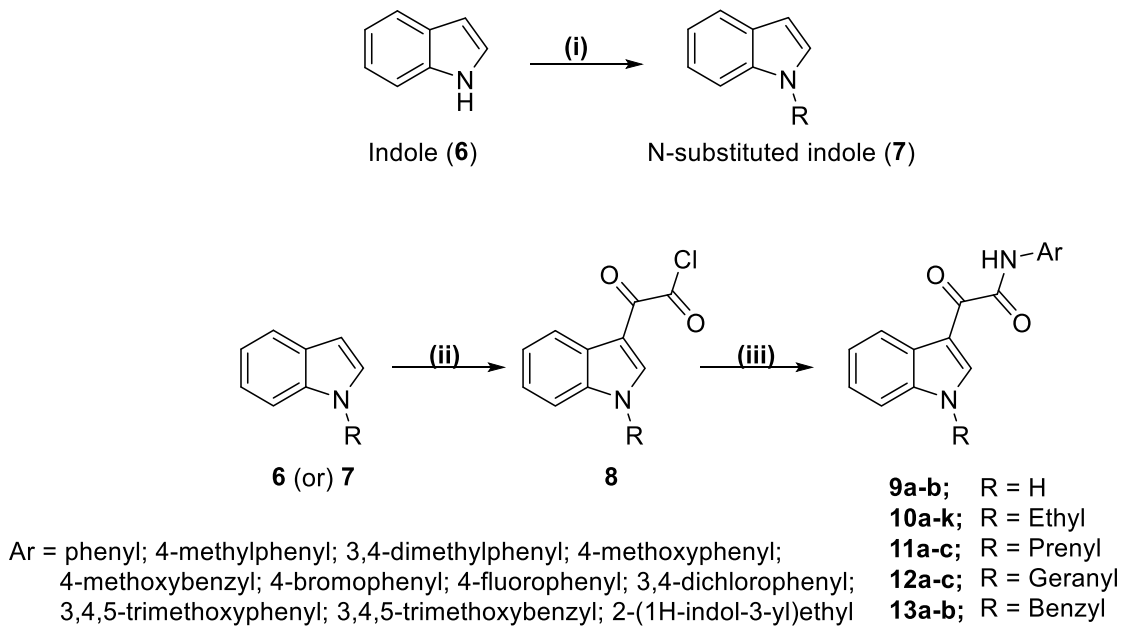

Scheme 1. Reagents and conditions: **(i)** Ethyl bromide/Benzyl chloride/Prenyl bromide/Geranyl bromide, KOH, DMF, RT, 12 h; **(ii)** $(COCl)_2$, Et_2O, 0 °C, 30 min; **(iii)** Ar-NH_2, TEA, THF, RT, 2 h.

The syntheses of all the final compounds (Table 1) were carried out as per the procedure detailed in Scheme 1.[10,16,18] Briefly, indole (**6**) was subjected to N-substitution with various halides in the presence of KOH as base. The N-benzylindole was obtained as crude precipitate and purified by recrystallization from ethanol. The N-ethyl, N-prenyl and N-geranyl indoles, obtained as oily liquids, were extracted using chloroform and purified through column

chromatography. Various indole analogues (**6** and **7**) were then allowed to react with oxalyl chloride under ice-cold conditions to afford the respective glyoxylyl chloride derivative **8** in good yields. Further, the reaction of **8** with various aniline derivatives in the presence of triethylamine afforded the final compounds in good yields (68-91%). All these analogues, with an exception of **9b** and **10k**, were synthesized for the first time (confirmed via SciFinder).

Structures of the synthesized analogues were well characterized using IR, NMR (^{1}H and ^{13}C) and HRMS. In the ^{1}H NMR, the -NH protons of amide functionality resonated at 10-11 ppm, while the proton at C_2 adjacent to the indole nitrogen resonated at 8-9 ppm. For analogues **10a-k,** the methyl protons of the N-ethyl substitution appeared as a triplet between 1-2 ppm, while the -CH_2 protons appeared as a quartet between 4-5 ppm. For the N-prenyl/N-geranyl substitutions, the terminal -CH_3 protons resonated at 1.5-2 ppm. For compounds **13a** and **13b**, the methylene protons of the N-benzyl substitution appeared as a singlet between 5-6 ppm. In ^{13}C NMR spectra, carbons of carbonyl and amide functionalities were resonated at ~180 (CO) and ~160 ppm (NHCO). In addition, for the compounds **11a-c**, the terminal methyl carbons of the N-prenyl substitution were observed around 18 and 25 ppm, while the -CH_2 carbon attached to the nitrogen of the indole resonated at 45 ppm. Similarly, for the compounds **12a-c**, the three methyl carbons as well as the carbons of the -CH_2-CH_2- linkers in the N-geranyl substitution resonated in between 16-40 ppm, while the -CH_2 carbon attached to the nitrogen of the indole resonated at 45 ppm.

2.2. PL inhibition assay and kinetics

The PL inhibitory activity of the synthesized indolyl oxoacetamides was evaluated as per the protocol standardized in our laboratory.[19] Porcine PL (Type II) was used as the enzyme with 4-nitrophenyl butyrate as a substrate, while orlistat (**1**) was the reference standard. As summarized in Table 1, the N-ethyl substituted (**10a-k**) and the unsubstituted (**9a, 9b**) indolyl oxoacetamides exhibited moderate to poor PL inhibitory activity, with their IC_{50} values varying between 16 - 40 µM. On the contrary, all the N-benzyl, N-prenyl and N-geranyl substituted compounds, exhibited potent activity with $IC_{50} \leq 5$ µM. Analogue **12c** that possessed N-geranyl substitution on indole and a 2-(1H-indol-3-yl)ethyl extension on the amide, exhibited the most potent activity against PL, with an IC_{50} of 2.95 µM. The standard drug, orlistat (**1**), comparatively possessed potent IC_{50} of 0.99 µM.

In order to further understand the nature of inhibition, analogues **12b** and **12c** were subjected to enzyme inhibition kinetics study, that in turn would provide adequate information

of the ligand's binding site.[20,21] For this, three concentrations each of **12b** and **12c** (0, 5 and 10 μM) were taken and the PL inhibition assay was performed against four different substrate concentrations (25, 50, 100 and 200 μM) to obtain a double reciprocal Lineweaver-Burk plot.

Table 1. *In vitro* PL inhibitory activity of indolyl oxoacetamides

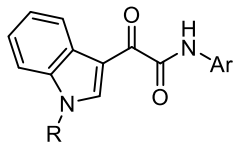

#	R	Ar	IC_{50} (μM)	#	R	Ar	IC_{50} (μM)
9a	H	3,4,5-trimethoxybenzyl	24.58 ± 1.62	**10j**	Ethyl	3,4,5-trimethoxybenzyl	18.42 ± 1.36
9b	H	2-(1*H*-indol-3-yl)ethyl	19.98 ± 1.92	**10k**	Ethyl	2-(1*H*-indol-3-yl)ethyl	16.04 ± 0.96
10a	Ethyl	phenyl	21.92 ± 2.18	**11a**	Prenyl	3,4,5-trimethoxyphenyl	5.48 ± 0.17
10b	Ethyl	4-methylphenyl	19.73 ± 2.01	**11b**	Prenyl	3,4,5-trimethoxybenzyl	4.15 ± 0.48
10c	Ethyl	3,4-dimethylphenyl	18.85 ± 1.88	**11c**	Prenyl	2-(1*H*-indol-3-yl)ethyl	3.72 ± 0.42
10d	Ethyl	4-methoxyphenyl	20.63 ± 2.16	**12a**	Geranyl	3,4,5-trimethoxyphenyl	3.99 ± 0.14
10e	Ethyl	4-methoxybenzyl	19.74 ± 0.38	**12b**	Geranyl	3,4,5-trimethoxybenzyl	3.26 ± 0.38
10f	Ethyl	4-bromophenyl	39.72 ± 2.46	**12c**	Geranyl	2-(1*H*-indol-3-yl)ethyl	2.95 ± 0.38
10g	Ethyl	3,4-dichlorophenyl	28.37 ± 1.72	**13a**	Benzyl	3,4,5-trimethoxybenzyl	4.26 ± 0.52
10h	Ethyl	4-fluorophenyl	37.68 ± 2.47	**13b**	Benzyl	2-(1*H*-indol-3-yl)ethyl	3.86 ± 0.49
10i	Ethyl	3,4,5-trimethoxyphenyl	17.24 ± 1.82	**4**	Benzyl	3,4,5-trimethoxyphenyl	4.92 ± 0.29

As represented in Figure 5, the convergence of the plots on the y-axis indicated that the analogues **12b** and **12c** inhibited PL competitively against the substrate similar to orlistat. Moreover, the K_m values increased proportionally with inhibitor concentration, while V_{max} remained constant (Table 2) clearly indicating that **12b** and **12c** exhibited reversible competitive inhibition. This fact is in line with our previous studies, wherein the indolyl oxoacetamides **4** and **5** also exhibited a reversible competitive inhibition of PL.[10,16] These results from the enzyme kinetics clearly highlighted the fact that analogues **12b** and **12c** bound to the active site of the PL, and exhibited inhibitory constant (K_i) value of 1.89 and 1.69 **μM, respectively, as calculated using the Cheng-Prusoff equation.**[22]

Table 2. K_m, V_{max} and K_i values of **12b** and **12c** retrieved from the enzyme kinetic study

Code	Km (in μM) at various concentrations of inhibitor			V_{max} (μM.min^{-1})	K_i (μM)
	0 μM	5 μM	10 μM		
12b	69.351	133.250	187.498	1.681	1.89
12c	67.14	133.79	184.52	1.549	1.69

View Article Online
DOI: 10.1039/D0NJ02622K

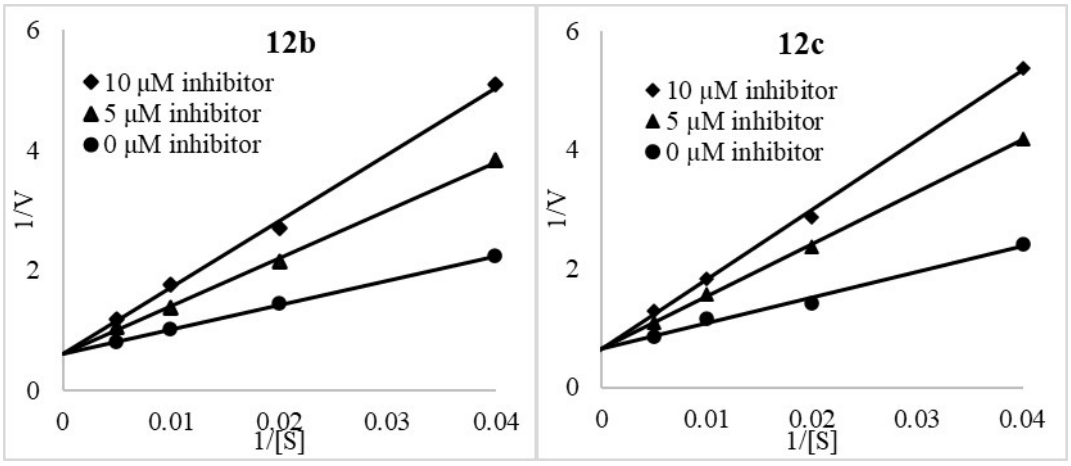

Fig. 5 Double reciprocal Lineweaver-Burk plots of **12b** and **12c** obtained through enzyme kinetic study

2.3. Structure activity relationship

A preliminary structure-activity relationship of the indolyl oxoacetamides with reference to their PL inhibitory activity is represented in Figure 6. For analogues **10a-i** that possessed an N-ethyl substitution on the indole, the presence of ring activating groups on the aryl ring of the amide nitrogen resulted in better potency, and is in line with our previous studies.[10,15,16] Further, the presence of 2-(1H-indol-3-yl)ethyl moiety on the amide (as seen with **11c**, **12c** and **13b**) resulted in better PL inhibitory potential, followed by the trimethoxybenzyl (**11b**, **12b** and **13a**) and trimethoxyphenyl moieties (**11a**, **12a** and **4**). Likewise, the presence of N-prenyl/N-geranyl/N-benzyl substitutions on the indole (**11a-c**, **12a-c** and **13a-b**, respectively) resulted in potent activity with IC_{50} values less than 5 µM, while the analogues with N-ethyl substitution (**10a-k**) and the N-unsubstituted analogues (**9a-b**) exhibited moderate to poor PL inhibitory activity. In particular, the presence of N-geranyl substitution (**12a-c**) has resulted in comparatively greater potency, and might be attributed to its greater hydrophobicity, leading to stronger hydrophobic interactions with the lid domain.

View Article Online
DOI: 10.1039/D0NJ02622K

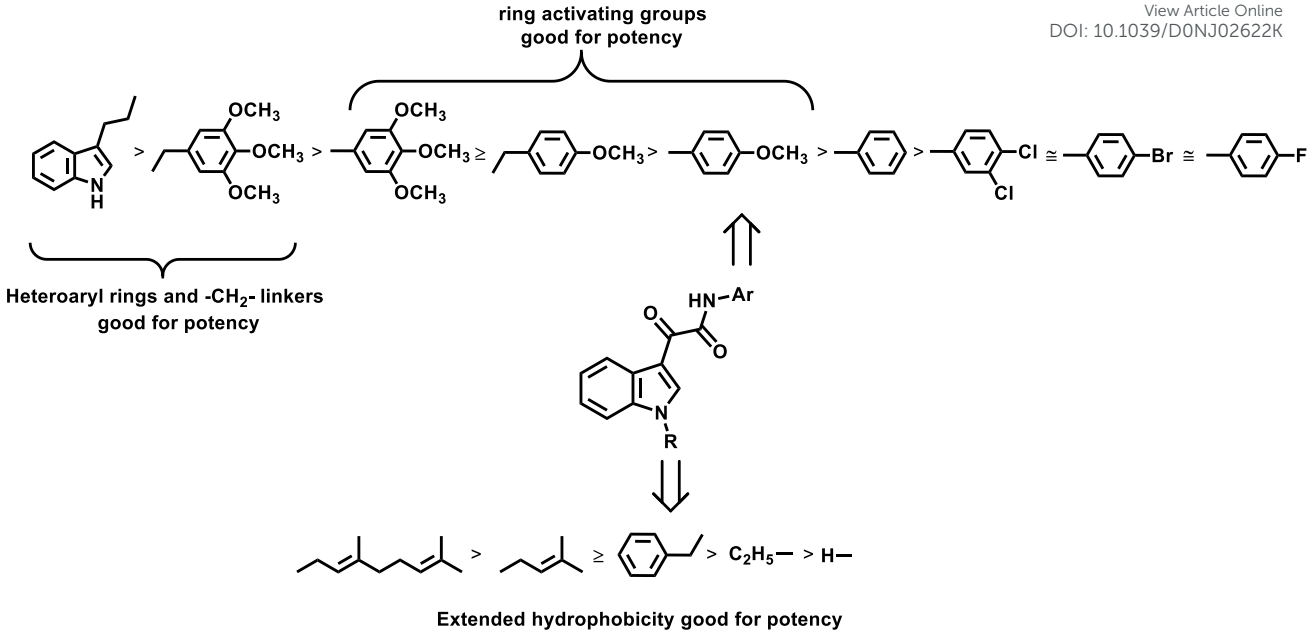

Fig. 6 Structure-activity relationship for indolyl oxoacetamides

2.4. Molecular docking and Molecular dynamics

Molecular docking studies of the indolyl oxoacetamides were performed using Molegro Virtual Docker 6.0, and the energy minimized structures of the ligands were docked in to the crystal structure of Human PL (PDB ID: 1LPB). A summary of the MolDock scores of the indolyl oxoacetamides with the active site of PL is represented in Table 3. The MolDock scores of the analogues exhibited significant correlation to their PL inhibitory activity (Pearson's r = 0.7658, $p < 0.05$), with the most potent analogue **12c** exhibiting potential MolDock score of -157.894 kcal/mol. Further, the MolDock scores of the N-benzyl, N-prenyl and the N-geranyl substituted analogues (**11a-c**, **12a-c** and **13a-b**) that exhibited potent IC_{50} values, possessed greater MolDock scores compared to a majority of the N-ethyl (**10a-i**) and the unsubstituted counterparts (**9a**).

Various interactions *viz.*, H-bond, π-π stacking, π-cation and alkyl hydrophobic interactions, exhibited by the indolyl oxoacetamides are summarised in Table 3. A majority of these analogues exhibited H-bond interactions with Phe 77 and His 263 among others. Further, the N-ethyl substituted analogues, with few exceptions, exhibited an additional H-bond interaction with Leu 153. On the contrary, the N-benzyl, N-prenyl and the N-geranyl substituted analogues exhibited additional H-bond interactions with Gly 76 (as seen with **11c**, **12a**, **13a)** and His 151 (as seen with **11c**, **12a**, **13a**, **13b**). Distinctively, analogue **12c** exhibited H-bond interaction with Ser 152 of the active site, which was not observed with other analogues

View Article Online
DOI: 10.1039/D0NJ02622K

(Figure 7). This Ser 152 forms the catalytic triad of the active site along with Asp 176 and His 263, and is involved in the hydrolysis of the triglyceride esters.[23]

The most common π-π stacking interactions exhibited by the indolyl oxoacetamides involved Tyr 114 and His 263, followed by Phe 77 and Phe 215. Moreover, all the analogues with few exceptions (**9a** and **13a**) exhibited intense alkyl interactions with various amino acids. In particular, the N-geranyl analogues (**12b** and **12c**) exhibited alkyl interactions with various amino acids of the lid domain *viz.*, Phe 77, Ile 78, Leu 213 and Phe 215. Previous literature suggests that the catalytic triad of the Human PL is enclosed in the lid domain (inactivated state), however, is activated by long alkyl chains of triglycerides through hydrophobic interactions with the lid domain amino acids.[24,25] These facts indicated that the N-geranyl substitution might act similar to these long alkyl chains in stabilization of open lid conformation, consequently leading to their better inhibitory potential.

Further, a contrasting variation was observed with the π-cation interactions exhibited by the oxoacetamides in the present study. As summarised in Table 3, the N-ethyl analogues, with exception for **10j** and **10k** did not exhibit interaction with Arg 256, which can be, in part, attributed to their poor PL inhibitory potential. Previous literature suggested that the open lid conformation of the Human PL is attained through formation of salt bridge between Arg 256-Asp 257 and Tyr 267-Lys 268.[26] Further, the role of π-cation interaction with Arg 256 in potentiating the activity was established in our previous studies.[10,15,16] Similar observations can be drawn with analogues **11c**, **12c** and **13b**, wherein the presence of 2-(1H-indol-3-yl)ethyl moiety with an ethylene linker might have resulted in better π-cation interaction with Arg 256, leading to their greater PL inhibitory potential. In comparison, the trimethoxybenzyl counterparts (**11b**, **12b** and **13a**) with a methylene linker exhibited lower inhibition followed by the trimethoxyphenyl counterparts (**11a**, **12a** and **4**) with no linker.

Molecular docking analysis clearly indicated the pivotal role of π-π stacking and alkyl interactions with the lid domain, as well as the π-cation interaction with Arg 256 in imparting potential PL inhibitory activity. In an attempt to better understand the role of these interactions, analogue **12c** was subjected to a 10 ns molecular dynamics (MD) simulation in complex with PL. As represented in Figure 8A, the backbone RMSD remained stable throughout the run, validating the MD simulation. Further, analogue **12c** remained stable in the active site during the first 3 ns, followed by a steep rise in RMSD from 2 Å to 3 Å (Figure 8B). However, the ligand remained stable through the rest of the 10 ns run, with a maximum deviation observed at 7 ns (RMSD ≈ 3.5 Å).

Table 3. MolDock scores (in kcal/mol) and the interactions of the indolyl oxoacetamides with the active site of Human PL

#	MolDock Score	H-bond	π-π stacking	π-cation interactions	Alkyl/π-alkyl interactions
9a	-128.723	Phe 77, His 263	Phe 77, Phe 215	Arg 256	Ile 78, Ala 178
9b	-138.285	Phe 77, Phe 215	Phe 215	Arg 256	Ala 178, Pro 180, Arg 256, Ala 259, Ala 260, Leu264
10a	-110.872	Phe 77, His 151, His 263	Tyr 114		Phe 77, Tyr 114, Ala 178, Pro 180, Ala 260
10b	-118.676	Phe 77, His 263	Tyr 114, His 263		Ala 178, Pro 180, Phe 215, Arg 256, Ala 260, Leu 264
10c	-121.694	Phe 77, His 263	Tyr 114, His 263		Ile 78, Ala 178, Pro 180, Phe 215, Arg 256, Ala 260, Leu 264
10d	-121.499	Phe 77, His 263	Tyr 114, His 263	Asp 79	Ile 78, Ala 178, Pro 180, Phe 215, Leu 264
10e	-117.877	Gly 76, Phe 77, Leu 153	Phe 77, Tyr 114, Phe 215	Asp 79	Tyr 114, Pro 180, Ile 209, Leu 264
10f	-123.105	Phe 77, Leu 153, His 263	Tyr 114, His 263		Phe 77, Ala 178, Pro 180, Phe 215, Arg 256, Leu 264
10g	-115.959	Phe 77, Leu 153, His 263	Tyr 114, His 263		Phe 77, Ala 178, Pro 180, Phe 215, Arg 256, Leu 264
10h	-119.34	Phe 77, His 263	Tyr 114, His 263		Ala 178, Pro 180, Phe 215, Ala 260, Leu 264
10i	-119.053	Phe 77, Leu 153, Arg 256	Phe 77, Tyr 114, Phe 215		Ala 178, Pro 180, Phe 215, Ala 260, Leu 264
10j	-136.352	Phe 77, Arg 256, His 263	Phe 77, Phe 215	His 263, Arg 256	Phe 77, Ile 78, Ala 178, Ala 260, Leu264
10k	-133.292	Phe 77, His 151, Leu 153, Arg 256, His 263	Phe 77	Arg 256	Ile 78, Ala 178, Phe 215, Ala 259, Ala 260, Leu 264
11a	-130.409	Phe 77, Leu 153	Phe 77	-	Phe 77, Ile 78, Ala 178, Pro 180, Phe 215, Leu 264
11b	-154.514	Phe 77, His 263	Phe 77, Phe 215	Arg 256	Ile 78, Ala 178, Phe 215, Ala 260, His 263
11c	-148.187	Gly 76, Phe 77, His 151, Leu 153	Phe 77	Arg 256, His 263	Phe 77, Ile 78, Ala 178, Ala 259, Ala 260, Leu264
12a	-156.058	Gly 76, Phe 77, His 151	Phe 77	Asp 79, His 263, Arg 256	Phe 77, Ile 78, Leu 153, Ala 178, Pro 180, Phe 215, Arg 256
12b	-153.101	Phe 77, Arg 256, His 263	Tyr 114, Phe 215	Arg 256	Phe 77, Ile 78, Ala 178, Pro 180, Ile 209, Leu 213, Phe 215
12c	-157.894	Phe 77, Ser 152	Tyr 114, His 263	Asp 79, Arg 256	Ile 78, Ala 178, Pro 180, Leu 213, Phe 215, Ala 259, Ala 260, Leu 264

13a	-135.654	Gly 76, Phe 77, His 151, Leu 153, Arg 256	Phe 77, Tyr 114, Phe 215	His 263, Arg 256	Ala 178, Ala 260, Leu 264
13b	-152.087	Phe 77, His 151, His 263	Phe 77	Arg 256, His 263	Ile 78, Ala 178, Ala 259, Ala 260, Leu264
Orlistat	-152.580	His 151, Ser 152	-	-	Tyr 114, Phe 215, Trp 252, Arg 256, Ala 259

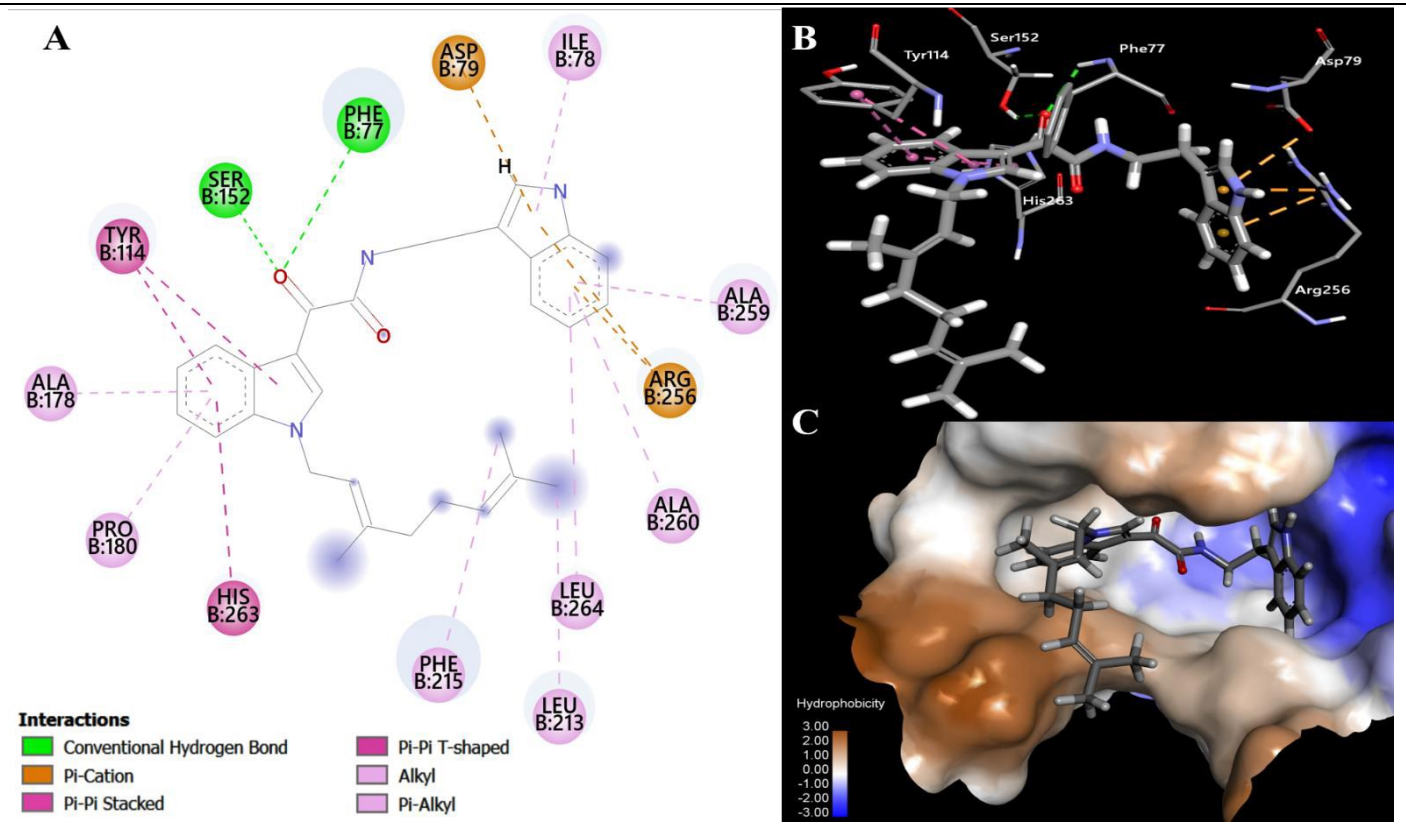

Fig. 7 (A) 2D interaction diagram of **12c** with PL; **(B)** 3D interaction diagram highlighting H-bond (green), π-π stacking (pink) and π-cation (brown) interactions of **12c** with the active site of PL; **(C)** Representation of **12c** in the binding pocket of PL, highlighting N-geranyl in close proximity with lid domain (in brown).

Table 4. Various interactions exhibited by **12c** during the 10 ns MD run

Frame	H-bond	π-π stacking	π-cation	Alkyl/π-alkyl interactions
0 ns	Asp 79	Phe 77, Phe 215	Arg 256	Ile 78, Tyr 114, Ala 178
1 ns	Phe 77	Phe 77, Tyr 114, Phe 215, Trp 252	-	Arg 256, Ala 259
2 ns	Asp 79	Phe 77, Phe 215	-	Ala 178, Ile 209, Val 210, Leu 213, Phe 215, Arg 256
3 ns	Ile 78	Phe 77, 215	Arg 256	Ile 78, Ala 178, Pro 180, Cys 181, Arg 256
4 ns	Asp 79, His 263	Phe 77, Tyr 114, Phe 215	-	Phe 77, Ile 78, Ala 178, Pro 180, Ile 209, Arg 256, Ala 259, Leu 264
5 ns	Asp 79	Phe 77, Tyr 114	Arg 256	Ile 78, Ala 259
6 ns	Asp 79	-	Arg 256	Ile 78, Arg 111
7 ns	Phe 77	His 263	-	Ile 78, Arg 111, Ala 259, Ala 260, Leu 264
8 ns	-	-	-	Ile 78, Arg 111, Arg 256, Ala 259, Ala 260, Leu 264
9 ns	-	-	-	Ile 78, Arg 256, Ala 259, Ala 260, Leu 264
10 ns	-	-		Ile 78, Ala 259, Ala 260

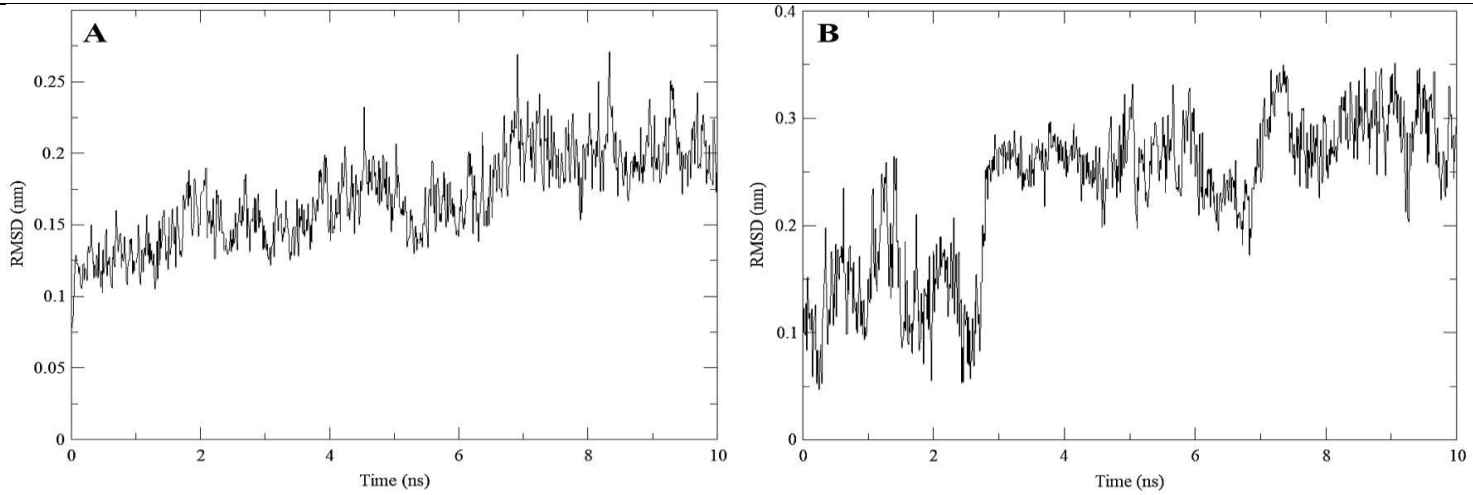

Fig. 8 Backbone RMSD (**A**) and ligand RMSD (**B**) retrieved from 10 ns MD simulation of **12c** - PL complex.

Various interactions exhibited by **12c** during the MD run are summarised in Table 4 and Figure 9. The ligand has maintained stable H-bond interactions with Asp 79 among others till 7 ns, beyond which all the H-bonds were lost. Similarly, **12c** exhibited stable π-π stacking and π-cation interactions with Phe 77, Tyr 114, Phe 215, and Arg 256, respectively, till 6 ns. However, **12c** exhibited stable alkyl interactions with various amino acids, including the lid domain, throughout the 10 ns MD run.

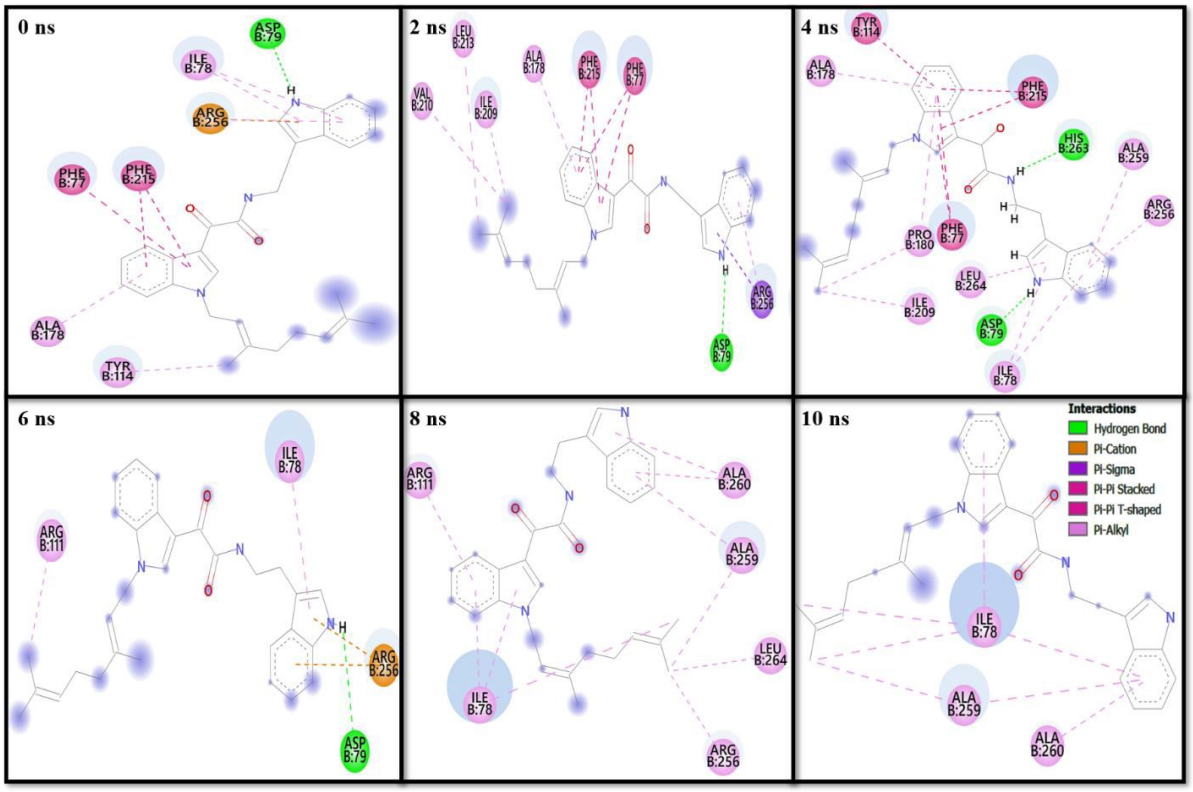

Fig. 9 2D representation of various interactions exhibited by **12c** with PL during the 10 ns MD simulation.

To summarize, an analysis of the molecular docking and molecular dynamics simulations in correlation to the PL inhibitory activity of the synthesized analogues, as well as the conclusions drawn from our previous studies[10,15,16] clearly highlighted the following attributes for a potent PL inhibition; a) highly reactive carbonyl group that can bind covalently to Ser 152 of the catalytic triad, b) strong π-π stacking interactions with the aromatic amino acids of the lid domain, *viz.*, Phe 77 and Phe 215, in addition to Tyr 114, c) additional alkyl/π-alkyl interactions with the lid domain amino acids, *viz.*, Gly 76 - Lys 80 and Leu 213 - Met 217, and d) strong π-cation interaction with Arg 256, the amino acid involved in the dynamics of the lid domain. Analogues **12b** and **12c** exhibited a majority of these interactions, however, lacked in π-π stacking with the lid domain. Further enhancement in its aromaticity might result in greater PL inhibitory activity.

View Article Online
DOI: 10.1039/D0NJ02622K

2.5. In silico ADMET prediction

The lipophilicity and ADMET (Absorption, Distribution, Metabolism, Excretion and Toxicity) profiles of the indolyl oxoacetamides in the present study were predicted using various tools *viz.*, SwissADME, ProTox-II and ToxTree,[27–29] and the results are summarized in Table 5. Orlistat (**1**) possessed comparatively higher LogP value and a low gastro-intestinal (GI) absorption which is in accordance with the reported data.[30] On contrary, all the indolyl oxoacetamides exhibited comparatively lower LogP values and high GI absorption. Nevertheless, the N-geranyl substituted analogues (**12a-c**) exhibited greater LogP (4.97-5.53) compared to conophylline (3.13) and the rest of the analogues (2.40-4.15). Similarly, analogues **12a** and **12b**, exhibited distribution and metabolism profiles similar to that of orlistat. However, all other analogues including **12c** were found to inhibit a majority of the CYP enzymes in contrast to orlistat.

For the toxicity profile, various parameters *viz.*, oral toxicity, carcinogenicity and hepatotoxicity were predicted. As summarised in Table 5, orlistat possessed a predicted LD_{50} of 1300 mg/kg (Class IV), and was also found to be genotoxic. Further, orlistat was predicted to be hepatotoxic, which is in line with the FDA reports.[31] On contrary, analogues **4** and **5** from the previous study possessed very low LD_{50} values (380 and 78 mg/kg, respectively), while also exhibiting hepatotoxicity similar to orlistat and conophylline. Nevertheless, the indolyl oxoacetamides in the present study were predicted to possess comparatively better toxicity profile, wherein all the analogues existed in Class IV for oral toxicity similar to orlistat and conophylline, but did not exhibit any carcinogenicity and hepatotoxicity.

Table 5. Lipophilicity and ADMET profile of the indolyl oxoacetamides

#	Lipophilicity	Absorption	Distribution		Metabolism					Toxicity			
					Inhibitor for					Oral	Carcinogenicity		Liver
	Consensus $LogP_{O/W}$	GI absorption	BBB permeant	P-gp substrate	CYP1A2	CYP2C19	CYP2C9	CYP2D6	CYP3A4	LD_{50} (mg/kg)	Genotoxic	Non-genotoxic	
9a	2.40	High	No	No	Yes	Yes	Yes	Yes	Yes	1000	No	No	No
9b, 13b	2.85	High	Yes	Yes	Yes	Yes	Yes	Yes	Yes	1000	No	No	No
10a-g	2.70 - 3.78	High	Yes	No	Yes	Yes	Yes	Yes	Yes	1000	No	No	No
10h	3.02	High	Yes	No	Yes	Yes	Yes	Yes	Yes	1000	No	No	No
10i	2.69	High	Yes	No	Yes	Yes	Yes	Yes	Yes	2000	No	No	No
10j	2.67	High	Yes	No	No	Yes	Yes	Yes	Yes	1000	No	No	No
10k	3.19	High	Yes	Yes	Yes	Yes	Yes	Yes	Yes	1000	No	No	No
11a	3.57	High	No	No	No	Yes	Yes	Yes	Yes	1000	No	No	No
11b	3.65	High	No	No	No	Yes	Yes	Yes	Yes	1000	No	No	No
11c	4.09	High	Yes	No	Yes	Yes	Yes	Yes	Yes	1000	No	No	No
12a	5.00	High	No	No	No	No	Yes	No	Yes	1000	No	No	No
12b	4.97	High	No	Yes	No	No	Yes	No	Yes	1000	No	No	No
12c	**5.53**	**High**	**No**	**Yes**	**Yes**	**Yes**	**Yes**	**Yes**	**Yes**	**1000**	**No**	**No**	**No**
13a	3.59	High	No	Yes	No	Yes	Yes	Yes	Yes	1000	No	No	No
13b	4.15	High	Yes	Yes	Yes	Yes	Yes	Yes	Yes	1000	No	No	No
Conophylline	3.13	Low	No	Yes	No	No	No	No	No	1190	Yes	No	Yes
4	3.62	High	No	No	Yes	No	Yes	Yes	Yes	380	No	No	Yes
5	3.56	High	No	No	Yes	No	Yes	Yes	Yes	78	No	No	Yes
Orlistat	**7.05**	**Low**	**No**	**Yes**	**No**	**No**	**Yes**	**No**	**No**	**1300**	**Yes**	**No**	**Yes**

View Article Online
DOI: 10.1039/D0NJ02622K

3. Conclusion

A series of 21 indolyl oxoacetamides were designed and synthesized as an attempt to optimize the lead **4** from our previous studies. These analogues were evaluated for their PL inhibitory activity, wherein analogues **12b** and **12c** possessed greater potential (IC_{50} values of 3.26 and 2.95 µM, respectively), compared to the natural product lead, conophylline (IC_{50} 3.31 µM). Further, five more analogues, **11b**, **11c**, **12a**, **13a** and **13b**, exhibited potent activity (< 5 µM). The MolDock scores of these analogues exhibited significant correlation to their PL inhibitory activity (Pearson's r = 0.7658, p < 0.05), with the most potent analogue **12c** exhibiting potential MolDock score of -157.894 kcal/mol. Further, a considerable improvement in the lipophilicity, in particular, for the N-geranyl substituted analogues (**12a**, **12b** and **12c**), resulted in extended hydrophobic interactions with the lid domain. Similarly, a heteroaryl ring (indol-3-yl), extended through an ethylene linker on the amide, also resulted in enhancement of the PL inhibitory activity. While the ADMET prediction of these analogues indicated a possible high GI absorption, the toxicity profile has indicated these analogues to be negative for carcinogenicity and hepatotoxicity, in contrary to orlistat and conophylline. In conclusion, the present study resulted in conophylline inspired novel indolyl oxoacetamides with potent pancreatic lipase inhibitory activity comparable to that of orlistat.

4. Materials and Methods

4.1. Chemistry

The synthesis of all the final analogues were carried out as per the procedure detailed in Scheme 1.[10,16,18] Progress of the reactions was followed by thin layer chromatography (TLC) analysis (Silica gel G60 F_{254}, Merck). Melting points were determined with electro thermal capillary melting point apparatus (*E-Z* melting) and are uncorrected. IR spectra were recorded on Shimadzu IRPrestige 21 FTIR machine using KBr pellets. ^{1}H and ^{13}C NMR spectra were recorded on a Bruker Avance II 400 spectrometer (400 MHz and 100 MHz, respectively) using DMSO-d_6 as solvent. HRMS analysis was performed on Bruker Compass Data Analysis 4.1 mass instrument. The purity of the synthesized compounds was determined on a Shimadzu SIL-20AC HT Ultra-Fast Liquid Chromatograph, equipped with SPD-20A UV detector. All

the compounds were through a Hypersil Gold column (Thermofisher, 250 mm x 4.6 mm with particle size of 5 µm) and the mobile phase used was Acetonitrile : Water (80 : 20% v/v).

4.1.1. General procedure for the synthesis of N-substituted indole (7)

Briefly, to 10 mL DMF taken in a 100 mL round bottomed flask, 25.6 mmol of KOH was added and stirred vigorously for 15 minutes at room temperature. To this, 8.5 mmol of indole (**6**) was added and the stirring was continued. After 30 minutes, a solution of appropriate halide (8.5 mmol in 5 mL DMF) was added dropwise for over 5 minutes to the reaction mixture, and the stirring was continued overnight. The reaction mixture was then transferred to ice-cold water. The N-benzyl substituted indole analogues were obtained as crude precipitates, and were purified by recrystallization. The N-ethyl, N-prenyl and N-geranyl substituted indoles were obtained as oily liquids, which were extracted using chloroform and purified through column chromatography.

4.1.2. General procedure for the synthesis of indolyl oxoacetamides

Various indole analogues (**6** and **7**, 2.5 mmol) were stirred at 0°C for 30 minutes in 5 mL diethylether. To this, oxalyl chlroide (2.5 mmol) was added dropwise for a period of over 5 min, and the reaction was continued at 0°C for 15 minutes. The obtained yellow precipitate of glyoxylyl chloride derivative (**8**) was filtered, washed with cold ether, and transferred immediately to a solution of THF containing appropriate amount of aniline derivative, followed by addition of triethylamine (7.5 mmol). The reaction was continued at room temperature for 2 hours, and THF was removed *in vacuo* to yield crude indolyl oxoacetamide. The crude precipitate was then re-crystallized from ethanol to obtain the final compounds in 68-91% yields.

*2-(1H-indol-3-yl)-2-oxo-N-(3,4,5-trimethoxybenzyl)acetamide (**9a**)*

Yield 81%; Brownish white solid; m.p: 239-241°C; ^{1}H NMR (400 MHz, DMSO-d_6) δ 12.25 (s, 1H, -NH of indole), 9.23 (t, J = 6.4 Hz, 1H, -NH of amide), 8.75 (s, 1H, H-2 of indole), 8.29-8.20 (m, 1H, H-4 of indole), 7.59-7.50 (m, 1H, H-5 of indole), 7.33-7.22 (m, 2H, H-6,7 of indole), 6.68 (s, 2H, H-2,6 of 3,4,5-trimethoxybenzyl), 4.38 (d, J = 6.3 Hz, 2H, -CH_2 linked to amide), 3.76 (s, 6H, 3 and 5-OCH_3), 3.64 (s, 3H, 4-OCH_3); ^{13}C NMR (100 MHz, DMSO-d_6) δ 182.7, 164.2, 153.2, 138.8, 136.9, 136.7, 135.0, 126.6, 123.9, 123.0, 121.7, 113.0, 112.6, 105.2, 60.4, 56.2, 42.7; IR (KBr, v, cm^{-1}) 3736, 2835, 2355, 2318, 2122, 1751, 1595, 1449,

1362, 1256, 1134, 988, 739, 689, 511; HRMS (ESI$^+$) calculated for $C_{20}H_{21}N_2O_5$ [M+H$^+$], 369.1372; Found 369.1398; HPLC Purity: 98.882%, t_R = 3.594 min.

*2-(1H-indol-3-yl)-2-oxo-N-(2-(1H-indol-3-yl)ethyl)acetamide (**9b**)*

Yield 87%; Creamy white solid; m.p: 221-223°C; ^{1}H NMR (400 MHz, DMSO-d_6) δ 12.22 (s, 1H, -NH of indole), 10.86 (s, 1H, -NH of 2-(indol-3-yl)ethyl), 8.86 (t, *J* = 6.0 Hz, 1H, -NH of amide), 8.79 (s, 1H, H-2 of indole), 8.25 (dt, *J* = 8.1, 2.8 Hz, 1H), 7.62 (d, *J* = 7.8 Hz, 1H), 7.55 (dt, *J* = 8.0, 2.9 Hz, 1H), 7.36 (d, *J* = 8.1 Hz, 1H), 7.33-7.19 (m, 3H), 7.09 (t, *J* = 7.5 Hz, 1H), 7.00 (t, *J* = 7.4 Hz, 1H), 3.57-3.50 (m, 2H, -CH_2 linked to amide), 2.97 (t, *J* = 7.6 Hz, 2H, -CH_2 of 2-(indol-3-yl)ethyl); ^{13}C NMR (100 MHz, DMSO-d_6) δ 182.6, 163.9, 139.0, 136.7, 127.6, 126.7, 123.8, 123.1, 122.9, 121.7, 118.7, 113.0, 112.6, 112.0, 111.8, 39.8, 39.7, 39.5, 39.3, 25.3; IR (KBr, *v*, cm^{-1}) 3611, 2922, 2355, 2324, 1792, 1412, 1327, 1256, 1128, 1007, 826, 810, 673; HRMS (ESI$^+$) calculated for $C_{20}H_{18}N_3O_2$ [M+H$^+$], 332.1321; Found 332.1398, HPLC Purity: 95.639%, t_R = 3.626 min.

*2-(1-ethyl-1H-indol-3-yl)-2-oxo-N-phenylacetamide (**10a**)*

Yield 87%; Creamy white solid; m.p: 111-113°C; ^{1}H NMR (400 MHz, DMSO-d_6) δ 10.71 (s, 1H, -NH of amide), 8.85 (s, 1H, H-2 of indole), 8.37-8.28 (m, 1H, H-4 of indole), 7.88 (d, *J* = 7.4 Hz, 2H, H-3,5 of phenyl), 7.74-7.64 (m, 1H, H-5 of indole), 7.44-7.30 (m, 4H), 7.15 (t, *J* = 7.4 Hz, 1H, H-4 of phenyl), 4.38 (q, *J* = 7.2 Hz, 2H, -CH_2 of ethyl), 1.43 (t, *J* = 7.2 Hz, 3H, -CH_3 of ethyl); ^{13}C NMR (100 MHz, DMSO-d_6) δ 181.9, 162.8, 140.9, 138.5, 136.5, 129.2, 127.3, 124.7, 124.1, 123.5, 121.9, 120.6, 111.7, 111.4, 41.9, 15.6; IR (KBr, *v*, cm^{-1}): 3823, 3291, 2689, 2355,2106, 1701, 1555, 1396, 1312, 1219, 1165, 866, 689; HRMS (ESI$^+$) calculated for $C_{18}H_{17}N_2O_2$ [M+H$^+$], 293.1212; Found 293.1278, HPLC Purity: 98.325%, t_R = 4.756 min.

*2-(1-ethyl-1H-indol-3-yl)-2-oxo-N-(p-tolyl)acetamide (**10b**)*

Yield 84%; Creamy white solid; m.p: 160-162°C; ^{1}H NMR (400 MHz, DMSO-d_6) δ 10.53 (s, 1H, -NH of amide), 8.84 (s, 1H, H-2 of indole), 8.37-8.28 (m, 1H, H-4 of indole), 7.79-7.72 (m, 2H, H-5,6 of indole), 7.72-7.63 (m, 1H, H-7 of indole), 7.41-7.29 (m, 2H, H-2,6 of 4-methylphenyl), 7.19 (d, *J* = 8.2 Hz, 2H, H-3,5 of 4-methylphenyl), 4.38 (q, *J* = 7.2 Hz, 2H, -CH_2 of ethyl), 2.30 (s, 3H, 4-Me of phenyl), 1.44 (t, *J* = 7.2 Hz, 3H, -CH_3 of ethyl); ^{13}C NMR (100 MHz, DMSO-d_6) δ 182.0, 162.5, 140.9, 136.5, 136.0, 133.7, 129.5, 127.3, 124.0, 123.5, 122.0, 120.6, 111.6, 111.5, 41.9, 15.5, 15.5; IR (KBr, *v*, cm^{-1}): 3792, 3277, 2978, 2405, 2318,

1935, 1838, 1614, 1377, 1312, 1219, 1043, 957, 829; HRMS (ESI^+) calculated for $C_{19}H_{19}N_2O_2$ [$M+H^+$], 307.1368; Found 307.1434, HPLC Purity: 98.236%, t_R = 5.156 min.

*2-(1-ethyl-1H-indol-3-yl)-2-oxo-N-(3,4-dimethylphenyl)acetamide (**10c**)*

Yield 81%; Creamy yellow solid; m.p: 147-149°C; ^1H NMR (400 MHz, DMSO-d_6) δ 10.53 (s, 1H), 8.86 (s, 1H), 8.36-8.27 (m, 1H), 7.73-7.64 (m, 2H), 7.56 (dd, *J* = 8.1, 2.3 Hz, 1H), 7.41-7.29 (m, 2H), 7.12 (d, *J* = 8.2 Hz, 1H), 4.38 (q, *J* = 7.2 Hz, 2H), 2.23 (s, 3H), 2.20 (s, 3H), 1.43 (t, *J* = 7.2 Hz, 3H); ^{13}C NMR (100 MHz, DMSO-d_6) δ 182.0, 162.5, 140.9, 136.8, 136.5, 136.2, 132.5, 130.0, 127.3, 124.0, 123.5, 121.9, 121.7, 118.1, 111.6 , 111.4, 41.9, 20.1, 19.3, 15.6; IR (KBr, *v*, cm^{-1}): 3686, 3312, 2355, 2299, 2106, 1680, 1574, 1504, 1381, 1219, 1184, 991, 789, 602; HRMS (ESI^+) calculated for $C_{20}H_{21}N_2O_2$ [$M+H^+$], 321.1525; Found 321.1599, HPLC Purity: 98.127%, t_R = 5.639 min.

*2-(1-ethyl-1H-indol-3-yl)- 2-oxo-N-(4-methoxyphenyl)acetamide (**10d**)*

Yield 73%; Yellowish green solid; m.p: 178-180°C; ^1H NMR (400 MHz, DMSO-d_6) δ 10.51 (s, 1H, -NH of amide), 8.89 (s, 1H, H-2 of indole), 8.34-8.26 (m, 1H, H-4 of indole), 7.73 (d, *J* = 8.4 Hz, 2H, H-2,6 of 4-methoxyphenyl), 7.72-7.63 (m, 1H, H-5 of indole), 7.41-7.29 (m, 2H, H-6,7 of indole), 7.19 (d, *J* = 8.2 Hz, 2H, H-3,5 of 4-methoxyphenyl), 4.37 (q, *J* = 7.1 Hz, 2H, $-CH_2$ of ethyl), 3.80 (s, 3H, $-OCH_3$), 1.44 (t, *J* = 7.1 Hz, 3H, $-CH_3$ of ethyl); ^{13}C NMR (100 MHz, DMSO-d_6) δ 182.0, 162.2, 156.3, 140.9, 136.4, 131.6, 127.3, 124.0, 123.5, 122.1, 122.0, 114.3, 111.6, 111.5, 55.6, 41.9, 15.5; IR (KBr, *v*, cm^{-1}): 3645, 3291, 2830, 2355, 2318, 1711, 1595, 1381, 1222, 1165, 1097, 1022, 851, 799, 673, 440; HRMS (ESI^+) calculated for $C_{19}H_{19}N_2O_3$ [$M+H^+$], 323.1317; Found 323.1386, HPLC Purity: 98.302%, t_R = 4.533 min.

*2-(1-ethyl-1H-indol-3-yl)-2-oxo-N-(4-methoxybenzyl)acetamide (**10e**)*

Yield 68%; Creamy white solid; m.p: 90-93°C; ^1H NMR (400 MHz, DMSO-d_6) δ 10.56 (t, *J* = 6.2 Hz, 1H, -NH of amide), 8.87 (s, 1H, H-2 of indole), 8.37-8.24 (m, 1H, H-4 of indole), 7.68 (d, *J* = 8.4 Hz, 2H, H-2,6 of 4-methoxybenzyl), 7.72-7.63 (m, 1H, H-5 of indole), 7.41-7.29 (m, 2H, H-6,7 of indole), 7.17 (d, *J* = 8.2 Hz, 2H, H-3,5 of 4-methoxyphenyl), 4.48 (d, *J* = 6.1 Hz, 2H, $-CH_2$- linked to amide), 4.37 (q, *J* = 7.1 Hz, 2H, $-CH_2$ of ethyl), 3.80 (s, 3H, 4-OCH_3), 1.44 (t, *J* = 7.1 Hz, 3H, $-CH_3$ of ethyl); ^{13}C NMR (100 MHz, DMSO-d_6) δ 182.0, 163.8, 158.7, 140.8, 136.4, 131.4, 129.2, 127.3, 123.9, 123.3, 122.0, 114.1, 111.6, 111.5, 55.5, 41.9, 41.8, 15.5; IR (KBr, *v*, cm^{-1}): 3736, 3343, 2355, 2334, 1842, 1736, 1504, 1468, 1362, 1184, 1028, 826, 673, 530, 440; HRMS (ESI^+) calculated for $C_{20}H_{21}N_2O_3$ [$M+H^+$], 337.1474; Found 337.1535, HPLC Purity: 87.899%, t_R = 4.282 min.

View Article Online
DOI: 10.1039/D0NJ02622K

*2-(1-ethyl-1H-indol-3-yl)-2-oxo-N-(4-bromophenyl)acetamide (**10f**)*

Yield 79%; Light yellow solid; m.p: 178-180°C; ^{1}H NMR (400 MHz, DMSO-d_6) δ 10.87 (s, 1H, -NH of amide), 8.84 (s, 1H, H-2 of indole), 8.36-8.27 (m, 1H, H-4 of indole), 7.86 (d, J = 8.9 Hz, 2H, H-2,6 of 4-bromophenyl), 7.74-7.64 (m, 1H, H-5 of indole), 7.58 (d, J = 8.9 Hz, 2H, H-3,5 of 4-bromophenyl), 7.41-7.30 (m, 2H, H-6,7 of indole), 4.38 (q, J = 7.2 Hz, 2H, -CH_2 of ethyl), 1.43 (t, J = 7.2 Hz, 3H, -CH_3 of ethyl); ^{13}C NMR (100 MHz, DMSO-d_6) δ 181.5, 162.8, 141.0, 137.9, 132.0, 127.3, 124.1, 123.6, 119.2, 116.5, 111.7, 100.8, 41.9, 15.5; IR (KBr, v, cm^{-1}): 3611, 3312, 2922, 2355, 2106, 1857, 1686, 1524, 1418, 1381, 1240, 1150, 1007, 773, 667; HRMS (ESI$^+$) calculated for $C_{18}H_{16}BrN_2O_2$ [M+H$^+$], 371.0317; Found 371.0377, HPLC Purity: 86.783%, t_R = 5.605 min.

*2-(1-ethyl-1H-indol-3-yl)-2-oxo-N-(3,4-dichlorophenyl)acetamide (**10g**)*

Yield 91%; Light yellow solid; m.p: 162-163°C; ^{1}H NMR (400 MHz, DMSO-d_6) δ 11.05 (s, 1H, -NH of amide), 8.88 (s, 1H, H-2 of indole), 8.35-8.26 (m, 2H, H-4,5 of indole), 7.84 (dd, J = 8.9, 2.4 Hz, 1H, H-6 of indole), 7.75-7.61 (m, 2H, H-7 of indole and H-2 of 3,4-dichlorophenyl), 7.42-7.30 (m, 2H, H-5,6 of 3,4-dichlorophenyl), 4.39 (q, J = 7.2 Hz, 2H, -CH_2 of ethyl), 1.43 (t, J = 7.2 Hz, 3H, -CH_3 of ethyl); ^{13}C NMR (100 MHz, DMSO-d_6) δ 181.0, 162.9, 141.2, 138.6, 136.5, 131.4, 131.1, 127.3, 126.2, 124.2, 123.6, 121.9, 121.9, 120.8, 111.7, 111.2, 41.9, 15.6; IR (KBr, v, cm^{-1}): 3844, 3567, 3327, 2972, 2355, 2112, 1695, 1574, 1402, 1219, 1134, 1007, 935, 814, 667; HRMS (ESI$^+$) calculated for $C_{18}H_{15}Cl_2N_2O_2$ [M+H$^+$], 361.0432; Found 361.0493, HPLC Purity: 90.746%, t_R = 6.451 min.

*2-(1-ethyl-1H-indol-3-yl)-2-oxo-N-(4-fluorophenyl)acetamide (**10h**)*

Yield 91%; Brown solid; m.p: 150-152°C; ^{1}H NMR (400 MHz, DMSO-d_6) δ 10.81 (s, 1H, -NH of amide), 8.85 (s, 1H, H-2 of indole), 8.36-8.27 (m, 1H, H-4 of indole), 7.96 – 7.85 (m, 2H, H-5,6 of indole), 7.74-7.65 (m, 1H, H-7 of indole), 7.41-7.30 (m, 2H, H-2,6 of 4-fluorophenyl), 7.29-7.18 (m, 2H, H-3,5 of 4-fluorophenyl), 4.38 (q, J = 7.2 Hz, 2H, -CH_2 of ethyl), 1.43 (t, J = 7.2 Hz, 3H, -CH_3 of ethyl); ^{13}C NMR (100 MHz, DMSO-d_6) δ 181.8, 162.6, 160.2, 157.8, 141.0, 136.5, 134.9, 127.3, 124.1, 123.5, 122.5, 121.9, 115.9, 111.7, 41.9, 15.6; IR (KBr, v, cm^{-1}) 3879, 3611, 3331, 2922, 2355, 2318, 2087, 1857, 1807, 1611, 1412, 1260, 1113, 1057, 814, 652; HRMS (ESI$^+$) calculated for $C_{18}H_{16}FN_2O_2$ [M+H$^+$], 311.1118; Found 311.1176, HPLC Purity: 91.492%, t_R = 4.718 min.

View Article Online
DOI: 10.1039/D0NJ02622K

*2-(1-ethyl-1H-indol-3-yl)-2-oxo-N-(3,4,5-trimethoxyphenyl)acetamide (**10i**)*

Yield 84%; Creamy yellow solid; m.p: 153-155°C; ^{1}H NMR (400 MHz, DMSO-d_6) δ 10.57 (s, 1H, -NH of amide), 8.93 (s, 1H, H-2 of indole), 8.38-8.29 (m, 1H, H-4 of indole), 7.73-7.65 (m, 1H, H-5 of indole), 7.40-7.32 (m, 4H), 4.40 (q, J = 7.2 Hz, 2H, -CH_2 of ethyl), 3.79 (s, 6H, 3 and 5-OCH_3), 3.34 (s, 3H, 4-OCH_3), 1.43 (t, J = 7.2 Hz, 3H, -CH_3 of ethyl); ^{13}C NMR (100 MHz, DMSO-d_6) δ 181.4, 162.2, 153.1, 141.1, 136.4, 135.6, 134.6, 127.4, 124.1, 123.5, 122.0, 111.6, 111.3, 98.4, 60.6, 56.2, 41.9, 15.6; IR (KBr, v, cm^{-1}) 3611, 3312, 2340, 2318, 2106, 1736, 1645,1574, 1412, 1234, 1128, 1007, 829, 652, 633; HRMS (ESI$^+$) calculated for $C_{21}H_{23}N_2O_5$ [M+H$^+$], 383.1529; Found 383.1600, HPLC Purity: 90.447%, t_R = 4.404 min.

*2-(1-ethyl-1H-indol-3-yl)-2-oxo-N-(3,4,5-trimethoxybenzyl)acetamide (**10j**)*

Yield 77%; Brownish white solid; m.p: 145-147°C; ^{1}H NMR (400 MHz, DMSO-d_6) δ 9.24 (t, J = 6.3 Hz, 1H, -NH of amide), 8.84 (s, 1H, H-2 of indole), 8.27 (dd, J = 6.5, 1.9 Hz, 1H, H-5 of indole), 7.66 (dd, J = 6.6, 1.5 Hz, 1H, H-6 of indole), 7.39-7.26 (m, 2H, H-4,7 of indole), 6.68 (s, 2H, H-2,6 of 3,4,5-trimthoxybenzyl), 4.41-4.28 (m, 4H, -CH_2 linked to amide and -CH_2 of ethyl), 3.76 (s, 6H, 3 and 5-OCH_3), 3.64 (s, 3H, 4-OCH_3), 1.41 (t, J = 7.2 Hz, 3H, -CH_3 of ethyl).; ^{13}C NMR (100 MHz, DMSO-d_6) δ 182.1, 164.0, 153.2, 140.7, 136.9, 136.4, 135.0, 127.3, 123.9, 123.4, 122.0, 111.7, 111.5, 105.2, 60.4, 56.2, 42.7, 41.8, 15.5; IR (KBr, v, cm^{-1}) 3723, 3601, 2901, 2355, 2318, 2106, 1717, 1589, 1396, 1240, 1184, 1128, 1007, 810, 689; HRMS (ESI$^+$) calculated for $C_{22}H_{25}N_2O_5$ [M+H$^+$], 397.1685; Found 397.1755, HPLC Purity: 94.475%, t_R = 4.053 min.

*2-(1-ethyl-1H-indol-3-yl)-2-oxo-N-(2-(1H-indol-3-yl)ethyl)acetamide (**10k**)*

Yield 80%; Creamy white solid; m.p: 168-170°C; ^{1}H NMR (400 MHz, DMSO-d_6) δ 10.86 (s, 1H, -NH of 2-(indol-3-yl)ethyl), 8.86 (t, J = 6.0 Hz, 1H, -NH of amide), 8.82 (s, 1H, H-2 of indole), 8.32-8.21 (m, 1H), 7.70-7.58 (m, 2H), 7.39-7.26 (m, 3H), 7.21 (d, J = 2.3 Hz, 1H), 7.08 (ddd, J = 8.1, 6.9, 1.2 Hz, 1H), 7.00 (ddd, J = 8.0, 7.0, 1.1 Hz, 1H), 4.35 (q, J = 7.3 Hz, 2H, -CH_2 of N-ethyl), 3.58-3.47 (m, 2H, -CH_2 linked to amide), 2.96 (t, J = 7.5 Hz, 2H, -CH_2 of 2-(indol-3-yl)ethyl), 1.41 (t, J = 7.2 Hz, 3H, -CH_3 of N-ethyl); ^{13}C NMR (100 MHz, DMSO-d_6) δ 182.2, 163.9, 140.8, 136.7, 136.4, 127.6, 127.3, 123.9, 123.3, 123.1, 122.0, 121.4, 118.7, 118.7, 112.0, 111.8, 111.6, 111.5, 41.8, 39.8, 25.3, 15.6; IR (KBr, v, cm^{-1}) 3611, 2922, 2355, 2324, 1792, 1412, 1327, 1256, 1128, 1007, 826, 810, 673; HRMS (ESI$^+$) calculated for $C_{22}H_{22}N_3O_2$ [M+H$^+$], 360.1634; Found 360.1710, HPLC Purity: 92.347%, t_R = 4.180 min.

2-(1-(3-methylbut-2-en-1-yl)-1H-indol-3-yl)-2-oxo-N-(3,4,5-trimethoxyphenyl)acetamide ***(11a)***

Yield 74%; Creamy yellow solid; m.p: 172-174°C; ^{1}H NMR (400 MHz, DMSO-d_6) δ 10.57 (s, 1H, -NH of amide), 8.89 (s, 1H, H-2 of indole), 8.36-8.28 (m, 1H, H-4 of indole), 7.64-7.55 (m, 1H, H-5 of indole), 7.39-7.30 (m, 4H), 5.43-5.35 (m, 1H), 4.98 (d, J = 7.0 Hz, 2H, -N-CH_2), 3.78 (s, 6H, 3- and 5-OCH_3), 3.66 (s, 3H, 4-OCH_3), 1.86 (s, 3H, -CH_3 of N-prenyl), 1.74 (s, 3H, -CH_3 of N-prenyl); ^{13}C NMR (100 MHz, DMSO-d_6) δ 181.4, 162.1, 153.1, 141.2, 137.4, 136.6, 134.6, 134.5, 127.5, 124.1, 123.6, 122.0, 119.6, 111.9, 111.3, 98.4, 60.6, 56.2, 45.1, 25.8, 18.4; IR (KBr, v, cm^{-1}) 3752, 2922, 2355, 2318, 2016, 1751, 1686, 1518, 1377, 1256, 1128, 1057, 829, 789, 683; HRMS (ESI$^+$) calculated for $C_{24}H_{27}N_2O_5$ [M+H$^+$], 423.1842; Found 423.1910, HPLC Purity: 84.224%, t_R = 5.326 min.

2-(1-(3-methylbut-2-en-1-yl)-1H-indol-3-yl)-2-oxo-N-(3,4,5-trimethoxybenzyl)acetamide ***(11b)***

Yield 79%; White solid; m.p: 179-181°C; ^{1}H NMR (400 MHz, DMSO-d_6) δ 9.25 (t, J = 6.3 Hz, 1H, -NH of amide), 8.80 (s, 1H, H-2 of indole), 8.32-8.24 (m, 1H, H-4 of indole), 7.62-7.53 (m, 1H, H-5 of indole), 7.32 (ddd, J = 6.5, 4.0, 1.7 Hz, 2H, H-6,7 of indole), 6.67 (s, 2H, H-2,6 of 3,4,5-trimethoxybenzyl), 5.38 (t, J = 7.0 Hz, 1H, -C=CH- of N-prenyl), 4.93 (d, J = 7.0 Hz, 2H, -CH_2 linked to amide), 4.36 (d, J = 6.3 Hz, 2H, -N-CH_2- of prenyl), 3.76 (s, 6H, 3 and 5-OCH_3), 3.64 (s, 3H, 4-OCH_3), 1.84 (s, 3H, -CH_3 of N-prenyl), 1.74 (s, 3H, -CH_3 of N-prenyl); ^{13}C NMR (100 MHz, DMSO-d_6) δ 182.0, 164.0, 153.2, 140.8, 137.7, 136.8, 136.6, 135.0, 127.3, 123.9, 123.4, 122.0, 119.4, 111.7, 111.6, 105.1, 60.4, 56.2, 44.9, 42.7, 25.8, 18.4; IR (KBr, v, cm^{-1}) 3773, 3474, 2922, 2355, 2318, 2127, 1680, 1412, 1256, 1165, 1134, 1007, 810, 689; HRMS (ESI$^+$) calculated for $C_{25}H_{29}N_2O_5$ [M+H$^+$], 437.1998; Found 437.2074, HPLC Purity: 89.895%, t_R = 4.704 min.

2-(1-(3-methylbut-2-en-1-yl)-1H-indol-3-yl)-2-oxo-N-(2-(1H-indol-3-yl)ethyl)acetamide ***(11c)***

Yield 83%; Light brown solid; m.p: 187-189°C; ^{1}H NMR (400 MHz, DMSO-d_6) δ 10.73 (s, 1H, -NH of 2-(indol-3-yl)ethyl), 8.89 (t, J = 6.1 Hz, 1H, -NH of amide), 8.76 (s, 1H, H-2 of indole), 8.32-8.21 (m, 1H), 7.72 (dd, J = 7.4, 1.5 Hz, 1H), 7.53 (dd, J = 7.4, 1.5 Hz, 1H), 7.31-7.22 (m, 3H), 7.21 (d, J = 2.3 Hz, 1H), 7.08 (ddd, J = 8.1, 6.9, 1.2 Hz, 1H), 7.00 (ddd, J = 8.0, 7.0, 1.1 Hz, 1H), 5.37-5.29 (m, 1H, -N-C-CH= of prenyl), 4.93 (d, J = 7.0 Hz, 2H, -N-CH_2 of prenyl), 3.58-3.47 (m, 2H, -CH_2 linked to amide), 2.96 (t, J = 7.5 Hz, 2H, -CH_2 of 2-(indol-3-

yl)ethyl), 1.84 (s, 3H, -CH_3 of N-prenyl), 1.74 (s, 3H, -CH_3 of N-prenyl); ^{13}C NMR (100 MHz, DMSO-d_6) δ 182.0, 163.7, 160.4, 140.9, 137.6, 136.7, 136.6, 127.6, 127.6, 127.4, 123.9, 123.3, 123.1, 123.0, 122.0, 121.4, 119.5, 118.7, 112.0, 44.9, 39.7, 25.8, 25.3, 25.2, 18.4; IR (KBr, *v*, cm^{-1}) 3595, 3299, 2355, 2318, 1611, 1499, 1381, 1256, 1128, 972, 814, 773, 689, 530; HRMS (ESI^+) calculated for $C_{25}H_{26}N_3O_2$ [$M+H^+$], 400.1947; Found 400.2017, HPLC Purity: 94.230%, t_R = 8.520 min.

*(E)-2-(1-(3,7-dimethylocta-2,6-dien-1-yl)-1H-indol-3-yl)-2-oxo-N-(3,4,5-trimethoxyphen yl)acetamide (**12a**)*

Yield 80%; Cream yellow solid; m.p: 86-88°C; ^{1}H NMR (400 MHz, DMSO-d_6) δ 10.57 (s, 1H, -NH of amide), 8.90 (s, 1H, H-2 of indole), 8.37-8.28 (m, 1H, H-4 of indole), 7.62-7.53 (m, 1H, H-5 of indole), 7.39-7.30 (m, 4H, H-6,7 of indole and H-2,6 of 3,4,5-trimethoxyphenyl), 5.37 (t, *J* = 6.8 Hz, 1H, -N-C-CH=), 5.06-4.95 (m, 3H), 3.78 (s, 6H, 3 and 5-OCH_3), 3.65 (s, 3H, 4-OCH_3), 2.11-1.99 (m, 4H), 1.85 (s, 3H, -CH_3 of N-geranyl), 1.55 (s, 3H, terminal -CH_3 of N-geranyl), 1.51 (s, 3H, terminal -CH_3 of N-geranyl); ^{13}C NMR (100 MHz, DMSO-d_6) δ 181.4, 162.1, 153.1, 141.2, 140.8, 136.7, 134.5, 131.5, 127.5, 124.0, 123.6, 121.9, 119.5, 111.9, 111.3, 99.9, 98.6, 98.4, 60.5, 56.2, 56.1, 45.0, 26.1, 25.8, 17.9, 16.6; IR (KBr, *v*, cm^{-1}) 3574, 3240, 2371, 2318, 1807, 1651, 1412, 1346, 1256, 1128, 1022, 845, 758, 637; HRMS (ESI^+) calculated for $C_{29}H_{35}N_2O_5$ [$M+H^+$], 491.2468; Found 491.2525, HPLC Purity: 79.412%, t_R = 8.928 min.

*(E)-2-(1-(3,7-dimethylocta-2,6-dien-1-yl)-1H-indol-3-yl)-2-oxo-N-(3,4,5-trimethoxybenzyl) acetamide (**12b**)*

Yield 72%; Yellowish white solid; m.p: 72-74°C; ^{1}H NMR (400 MHz, DMSO-d_6) δ 9.26 (t, *J* = 6.3 Hz, 1H, -NH of amide), 8.81 (s, 1H, H-2 of indole), 8.32-8.24 (m, 1H, H-4 of indole), 7.62- 7.53 (m, 1H, H-5 of indole), 7.36-7.31 (m, 2H, H-6,7 of indole), 6.66 (s, 2H, H-2,6 of 3,4,5-trimethoxybenzyl), 5.06-4.95 (m, 3H, -N-CH_2-CH= of geranyl), 4.36 (d, *J* = 6.3 Hz, 2H, -CH_2 linked to amide), 3.78 (s, 6H, 3 and 5-OCH_3), 3.65 (s, 3H, 4-OCH_3), 2.11-1.99 (m, 2H), 2.06-2.01 (m, 3H), 1.87 (s, 3H, -CH_3 of N-geranyl), 1.56 (s, 3H, terminal -CH_3 of N-geranyl), 1.52 (s, 3H, terminal -CH_3 of N-geranyl); ^{13}C NMR (100 MHz, DMSO-d_6) δ 182.0, 163.9, 153.2, 140.9, 140.9, 136.8, 136.6, 135.0, 131.5, 127.4, 124.0, 123.9, 123.4, 121.9, 119.4, 111.8, 111.6, 105.1, 60.4, 56.2, 44.9, 42.7, 26.1, 25.8, 17.9, 16.6; IR (KBr, *v*, cm^{-1}) 3736, 3331, 2851, 2318, 1751, 1611, 1504, 1472, 1377, 1234, 1134, 922, 814, 633; HRMS (ESI^+) calculated for $C_{30}H_{37}N_2O_5$ [$M+H^+$], 505.2624; Found 505.2695, HPLC Purity: 94.219%, t_R = 7.311 min.

*(E)-2-(1-(3,7-dimethylocta-2,6-dien-1-yl)-1H-indol-3-yl)-2-oxo-N-(2-(1H-indol-3-yl)ethyl) acetamide (**12c**)*

Yield 69%; Light brown solid; m.p: 93-95°C; ^{1}H NMR (400 MHz, DMSO-d_6) δ 10.87 (s, 1H, -NH of 2-(indol-3-yl)ethyl), 8.86 (t, *J* = 6.0 Hz, 1H, -NH of amide), 8.82 (s, 1H, H-2 of indole), 8.31-8.22 (m, 1H), 7.61 (d, *J* = 7.9 Hz, 1H), 7.58-7.53 (m, 1H), 7.39-7.25 (m, 3H), 7.20 (d, *J* = 2.3 Hz, 1H), 7.12-7.02 (m, 1H), 6.99 (td, *J* = 7.5, 7.0, 1.1 Hz, 1H), 5.36 (t, *J* = 6.6 Hz, 1H, -N-C-CH= of geranyl), 5.07-4.98 (m, 1H), 4.94 (d, *J* = 7.0 Hz, 2H, -N-CH_2 of geranyl), 3.51 (dt, *J* = 8.1, 6.4 Hz, 2H, -CH_2 linked to amide), 2.95 (t, *J* = 7.6 Hz, 2H, -CH_2 of 2-(indol-3-yl)ethyl), 2.11-2.01 (m, 4H), 1.84 (s, 3H, -CH_3 of N-geranyl), 1.56 (s, 3H, -CH_3 of N-geranyl), 1.52 (s, 3H, -CH_3 of N-geranyl); ^{13}C NMR (100 MHz, DMSO-d_6) δ 182.0, 163.7, 141.0, 140.8, 136.7, 136.6, 131.5, 127.6, 127.4, 125.3, 124.0, 123.8, 123.3, 123.1, 122.0, 121.4, 119.4, 118.7, 112.0, 111.8, 111.7, 111.6, 44.9, 34.8, 30.8, 26.7, 25.8, 25.3, 18.0, 16.6; IR (KBr, *v*, cm^{-1}) 3630, 3296, 2866, 2355, 2303, 1802, 1696, 1362, 1256, 1128, 1007, 951, 814, 779, 673; HRMS (ESI$^+$) calculated for $C_{30}H_{34}N_3O_2$ [M+H$^+$], 468.2573; Found 468.2642, HPLC Purity: 95.948%, t_R = 7.847 min.

*2-(1-benzyl-1H-indol-3-yl)-2-oxo-N-(3,4,5-trimethoxybenzyl)acetamide (**13a**)*

Yield 73%; Yellowish white solid; m.p: 167-169°C; ^{1}H NMR (400 MHz, DMSO-d_6) δ 9.27 (t, *J* = 6.3 Hz, 1H, -NH of amide), 8.99 (s, 1H, H-2 of indole), 8.33-8.24 (m, 1H, H-4 of indole), 7.65-7.56 (m, 1H, H-5 of indole), 7.39-7.24 (m, 7H, H-6,7 of indole and aromatic protons of N-benzyl), 6.68 (s, 2H, H-2,6 of 3,4,5-trimethoxybenzyl), 5.60 (s, 2H, -CH_2 of N-benzyl), 4.38 (d, *J* = 6.3 Hz, 2H, -CH_2 linked to amide), 3.76 (s, 6H, 3 and 5-OCH_3), 3.64 (s, 3H, 4-OCH_3); ^{13}C NMR (100 MHz, DMSO-d_6) δ 182.3, 163.9, 153.2, 141.6, 137.1, 136.9, 136.7, 135.7, 135.0, 129.2, 128.2, 127.8, 127.3, 124.1, 123.4, 122.0, 112.0, 105.2, 60.4, 56.2, 50.2, 42.7; IR (KBr, *v*, cm^{-1}) 3736, 3418, 2953, 2374, 2318, 1857,1792, 1464, 1306, 1128, 1043, 814, 795, 474; HRMS (ESI$^+$) calculated for $C_{27}H_{27}N_2O_5$ [M+H$^+$], 459.1842; Found 459.1907, HPLC Purity: 98.649%, t_R = 4.402 min.

*2-(1-benzyl-1H-indol-3-yl)-2-oxo-N-(2-(1H-indol-3-yl)ethyl)acetamide (**13b**)*

Yield 76%; Brown solid; m.p: 187-189°C; ^{1}H NMR (400 MHz, DMSO-d_6) δ 10.73 (s, 1H, -NH of 2-(indol-3-yl)ethyl), 9.07 (s, 1H, -NH of amide), 8.89 (s, 1H, H-2 of indole), 8.69 (dd, *J* = 7.4, 1.4 Hz, 1H), 7.62 (dd, *J* = 7.5, 1.5 Hz, 1H), 7.53 (dd, *J* = 7.3, 1.5 Hz, 1H), 7.38-7.23 (m, 7H), 7.16 (s, 1H), 7.06 (m, 2H), 7.02-6.94 (m, 1H), 5.56 (s, 2H, -CH_2 of N-benzyl), 3.49 (t, *J* = 5.4 Hz, 2H, -CH_2 linked to amide), 2.81 (t, *J* = 5.4 Hz, 2H, -CH_2 of 2-(indol-3-yl)ethyl);

^{13}C NMR (100 MHz, DMSO-d_6) δ 183.0, 165.7, 137.2, 136.5, 135.0, 134.6, 129.5, 128.0, 127.6, 126.7, 123.9, 122.6, 122.2, 122.1, 121.2, 119.4, 118.7, 115.9, 112.5, 111.4, 110.8, 51.5, 40.4, 26.0; IR (KBr, ν, cm^{-1}) 3611, 2922, 2355, 2324, 1792, 1412, 1327, 1256, 1128, 1007, 826, 810, 673; HRMS (ESI$^+$) calculated for $C_{27}H_{24}N_3O_2$ [M+H$^+$], 422.1790; Found 422.1862, HPLC Purity: 79.639%, t_R = 4.566 min.

4.2. Pancreatic lipase inhibition assay and enzyme kinetics

Orlistat (**1)**, Porcine PL (Type II) and 4-nitrophenyl butyrate were procured from Sigma-Aldrich (MO, USA). Tris buffer and sodium chloride (molecular biology grade) were procured from Sisco Research Laboratories (MH, India). All other chemicals and solvents (analytical grade) were used without further purification.

The procedure for PL inhibition assay and kinetics was performed as per the protocol standardized in our laboratory.[19] Briefly, a suspension of porcine pancreatic lipase (5 mg/mL) was subjected to vigorous shaking, followed by centrifugation (4000 rpm, 10 min), and the supernatant was used afresh as the enzyme solution. Stock solutions of the synthesized compounds and orlistat (**1)** were prepared in DMSO at linear concentrations ranging from 0.78 - 2000 µg/mL. The final reaction mixture comprised of 875 µL of buffer, 100 µL of enzyme and 20 µL of the compounds of various stock concentrations, pre-incubated for 5 min at 37 °C, followed by addition of 5 µL of the substrate (4-nitrophenyl butyrate, 10 mM in acetonitrile). The absorbance of the final mixture was taken on a BioTek EPOCH microplate spectrophotometer (VT, USA) after 5 min at absorbance maxima of 4-nitrophenol (405 nm). The assay was performed in triplicate and the percentage inhibition was calculated using the formula

$$\% \text{ inhibition} = [1-(A_T / A_E)] \times 100$$

where A_E is the absorbance of enzyme control (without inhibitor), and A_T is the difference between the absorbance of test sample, with and without substrate. The IC_{50} of the compounds was calculated by plotting linear regression curve.

For the inhibition kinetics, the assay protocol was repeated with varying concentrations of **12b** and **12c** (0, 5 and 10 µM) and substrate (25, 50, 100 and 200 µM), and a double reciprocal Lineweaver-Burk plot was plotted to understand the nature of inhibition.[32] The inhibition constant, K_i, was calculated from Cheng-Prusoff equation.[22]

View Article Online
DOI: 10.1039/D0NJ02622K

4.3. Molecular modelling studies

Molecular docking of the indolyl oxoacetamides was performed using Molegro Virtual Docker 6.0.[33] Prior to docking, all the ligands were subjected to energy minimization using Molecular Mechanics 2 (MM2) force field in Chem3D module of ChemBioOffice v12 (PerkinElmer, USA). The crystal structure of Human PL (PDB ID: 1LPB) was retrieved from the RCSB PDB Data bank,[23] and the energy minimized ligands were docked in to the active site using previously validated grid parameters.[16]

Molecular dynamics (MD) simulation of compound **12c** in complex with PL was performed as per the protocol standardized in our laboratory.[10,16] Gromacs 5.0.4, compiled on a CentOS 7 operating system equipped with Intel(R) Xeon(R) CPU W3565 and NVIDIA Quadro 4000 Quad-Core Processor was used for the purpose of MD simulation.[34] CHARMM27 force field[35] was applied during the MD run, and the topology of the ligand **12c** was generated using online tool provided by Swiss Institute of Bioinformatics.[36] Prior to the initiation of the MD, the complex was minimized using Steepest Descent algorithm for 1000 steps, followed by stabilization of the system to 310 K and 1 atm pressure for 50 ps, using the canonical NVT and NPT ensembles. Parameters like Particle Mesh Ewald method for long-range electrostatics,[37] and 14 Å cut-off for van der Waals and columbic interactions were set during the MD simulation. LINCS algorithm was applied for the calculation of bond length.[38] Discovery Studio 4.5 visualizer (Accelrys, USA) was used to depict the graphical representations of the complex.

4.4. ADMET prediction

The *in silico* ADMET prediction of the synthesized analogues alongside orlistat (**1**), conophylline (**2**) and the indolyl oxoacetamides (**4** and **5**) was generated using various online tools and freeware *viz.*, SwissADME, ProTox-II and ToxTree (v 3.1.0). Parameters such as consensus $LogP_{O/W}$, GI absorption, blood-brain barrier (BBB) permeability and effect on CYP enzymes were predicted using SwissADME.[27] Toxicity parameters including oral toxicity (predicted as LD_{50}) and Hepatotoxicity were predicted using ProTox-II,[28] while carcinogenicity parameters *viz.*, Genotoxicity and Non-genotoxicity were predicted using ToxTree.[29]

5. Acknowledgements

View Article Online
DOI: 10.1039/D0NJ02622K

The authors acknowledge Birla Institute of Technology and Science, Pilani (BITS Pilani), Pilani Campus, Pilani, Rajasthan, India for providing NMR and other necessary laboratory facilities. The authors also acknowledge Department of Science and Technology (DST), New Delhi, India for sponsoring HR-MS facility at BITS Pilani under FIST program. Dr. S N C Sridhar acknowledges the Council for Scientific and Industrial Research (CSIR), New Delhi, India for providing fellowship (SRF - File No: 09/719 (0088)/2018-EMR-I).

6. Conflicts of Interest: There are no conflicts to declare.

7. References

1 S. M. Grundy, *Am. J. Clin. Nutr.*, 1998, **67**, 563S–572S.

2 WHO | Obesity. http://www.who.int/topics/obesity/en/ (Last accessed 12 May 2020).

3 G. A. Bray, K. K. Kim and J. P. H. Wilding, *Obes. Rev.*, 2017, **18**, 715–723.

4 WHO | Obesity and overweight. http://www.who.int/mediacentre/factsheets/fs311/en/ (Last accessed 12 May 2020).

5 L. Khaodhiar, K. C. McCowen and G. L. Blackburn, *Clin. Cornerstone*, 1999, **2**, 17–31.

6 S. N. C. Sridhar, G. George, A. Verma and A. T. Paul, in *Natural Bio-Active Compounds Volume 1: Production and Applications*., ed. M. S. Akhtar, M. K. Swamy and U. R. Sinniah, Springer Singapore, 2019, 6, 149–191.

7 D. Patel, *Metab. Exp.*, 2015, **64**, 1376–1385.

8 U.S. National Library of Medicine | Orlistat: MedlinePlus Drug Information. https://www.nlm.nih.gov/medlineplus/druginfo/meds/a601244.html#side-effects (Last accessed 12 May 2020).

9 USFDA | Safety Information>Xenical (orlistat) capsules. https://wayback.archive-it.org/7993/20170112172652/http://www.fda.gov/Safety/MedWatch/SafetyInformation/ucm215504.htm (Last accessed 12 May 2020).

10 D. Chauhan, G. George, S. N. C. Sridhar, R. Bhatia, A. T. Paul and V. Monga, *Arch. Pharm. (Weinheim).*, 2019, **352**, e1900029.

11 A. Stefanucci, M. P. Dimmito, G. Zengin, G. Luisi, S. Mirzaie, E. Novellino and A. Mollica, *New J. Chem.*, 2019, **43**, 3208–3217.

12 A. Stefanucci, G. Luisi, G. Zengin, G. Macedonio, M. P. Dimmito, E. Novellino and A. Mollica, *Future Med. Chem.*, 2019, **11**, 5–19.

13 S. N. C. Sridhar, S. Mutya and A. T. Paul, *Med. Chem. Res.*, 2017, **26**, 1268–1278.

14 S. N. C. Sridhar, P. Sengupta and A. T. Paul, *Ind. Crops Prod.*, 2018, **111**, 462–470.

15 S. N. C. Sridhar, G. Ginson, P. O. Venkataramana Reddy, M. P. Tantak, D. Kumar and A. T. Paul, *Bioorg. Med. Chem.*, 2017, **25**, 609–620.

16 S. N. C. Sridhar, S. Palawat and A. T. Paul, *Bioorg. Chem.*, 2019, **85**, 373–381.

17 Q. S. Du, J. Z. Meng, S. M. Liao and R. B. Huang, *J. Mol. Graph. Model.*, 2012, **34**, 38–45.

18 F. Naaz, M. C. P. Pallavi, S. Shafi, N. Mulakayala, M. S. Yar and H. M. S. Kumar, *Bioorg. Chem.*, 2018, **81**, 1–20.

19 S. N. C. Sridhar, D. Bhurta, D. Kantiwal, G. George, V. Monga and A. T. Paul, *Bioorg. Med. Chem. Lett.*, 2017, **27**, 3749–3754.

20 B. Ring, S. A. Wrighton and M. Mohutsky, *Enzym. Kinet. Drug Metab. Fundam. Appl.*, 2014, **1113**, 37–56.

21 P. K. Robinson, *Essays Biochem.*, 2015, **59**, 1–41.

22 B. T. Burlingham and T. S. Widlanski, *J. Chem. Educ.*, 2003, **80**, 214.

23 M. P. Egloff, F. Marguet, G. Buono, R. Verger, C. Cambillau and H. van Tilbeurgh, *Biochemistry*, 1995, **34**, 2751–2762.

24 F. K. Winkler, A. D'Arcy and W. Hunziker, *Nature*, 1990, **343**, 771–774.

25 H. van Tilbeurgh, M.-P. Egloff, C. Martinez, N. Rugani, R. Verger and C. Cambillau, 1993, **362**, 814–820.

26 M. E. Lowe, *J. Lipid Res.*, 2002, **43**, 2007–2016.

27 A. Daina, O. Michielin and V. Zoete, *Sci. Rep.*, 2017, **7**, 42717.

28 P. Banerjee, A. O. Eckert, A. K. Schrey and R. Preissner, *Nucleic Acids Res.*, 2018, **46**, W257-W263.

29 R. Benigni and others, *JRC Sci. Tech. Reports*, 2008, 1–78.

30 XENICAL® (orlistat) CAPSULES. https://www.accessdata.fda.gov/drugsatfda_docs/label/2010/020766s028lbl.pdf (Last accessed 12 May 2020).

31 FDA Drug Safety Communication: Completed safety review of Xenical/Alli (orlistat) and severe liver injury. https://www.fda.gov/drugs/postmarket-drug-safety-information-patients-and-providers/fda-drug-safety-communication-completed-safety-review-xenicalalli-orlistat-and-severe-liver-injury (Last accessed 12 May 2020).

32 H. Lineweaver and D. Burk, *J. Am. Chem. Soc.*, 1934, **56**, 658–666.

33 R. Thomsen and M. H. Christensen, *J. Med. Chem.*, 2006, **49**, 3315–3321.

34 M. J. Abraham, D. Van Der Spoel, E. Lindahl and B. Hess, 2014.

35 A. D. MacKerell, N. Banavali and N. Foloppe, *Biopolymers*, 2000, **56**, 257–265.

36 V. Zoete, M. A. Cuendet, A. Grosdidier and O. Michielin, *J. Comput. Chem.*, 2011, **32**, 2359–2368.

37 T. Darden, D. York and L. Pedersen, *J. Chem. Phys.*, 1993, **98**, 10089–10092.

38 B. Hess, H. Bekker, H. J. C. Berendsen and J. G. E. M. Fraaije, *J. Comput. Chem.*, 1997, **18**, 1463–1472.

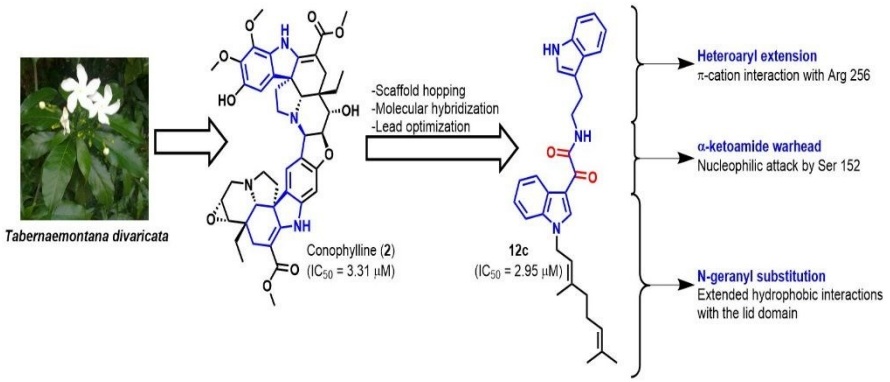

Twenty-one indolyl oxoacetamides were designed and synthesized inspired by conophylline. Analogues **12c** and **12b** with N-geranyl substitution on indole exhibited potent pancreatic lipase inhibition.